CHAPTER 10

GEOTECHNICAL DESIGN OF DRIVEN PILES UNDER AXIAL LOADS

10.1 COMMENT ON THE NATURE OF THE PROBLEM

Piles are generally used for two purposes: (1) to increase the load-carrying capacity of the foundation and (2) to reduce the settlement of the foundation. These purposes are accomplished by transferring loads through a soft stratum to a stiffer stratum at a greater depth, or by distributing loads through the stratum by friction along the pile shaft, or by some combination of the two. The manner in which the load is distributed from the pile to the supporting soil is of interest. A typical curve of the distribution of load along the length of an axially loaded pile is shown in Figure 10.1. This transfer of loads is extremely complex, highly indeterminate, and difficult to quantify analytically.

The method of pile installation is one of the important factors that affect load transfer between the pile and the supporting soil layers. Current construction practice for installation of piles may be divided into three basic categories: driving, boring, and jetting/vibrating. Driven piles are open-ended or closed-ended steel pipes, steel H-shapes, timber piles, or precast concrete piles driven by various types of driving hammers to the desired penetration for the required load-carrying capacity. This chapter focuses on the load-carrying capacity (also known as the *geotechnical capacity*) of driven piles only.

Computing the capacity of a single driven pile under axial loading is by no means a straightforward exercise. In practice, pile foundations have typically been designed based on either the pile-driving formula or the static formula. The static formula is considered the more reliable of the two. With this formula, the pile capacity is based on the static soil resistance determined

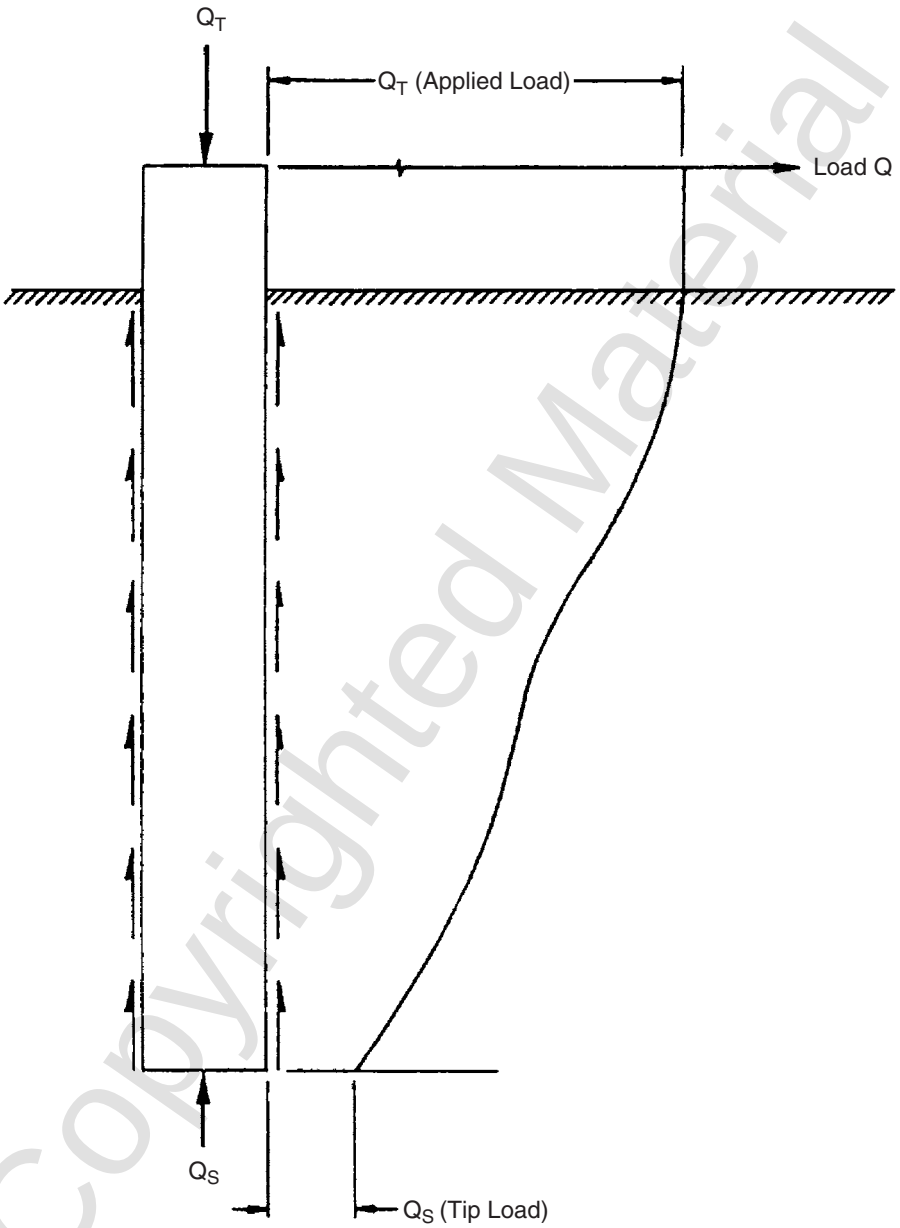

Figure 10.1 Curve showing the typical distribution of a load along the length of an axially loaded pile.

by the limit equilibrium theory for the tip of the pile and load transfer along the sides of the pile, termed *side resistance.* In discussing piles under axial load, the term *skin friction* has long been used to indicate the load along the sides of a pile. This term has a direct application to piles in granular soils but not to piles in cohesive soils, where *side resistance* is more descriptive. For piles in cohesive soils, because of traditional usage, *skin friction* is also used in some instances. The soil parameters used in the static formula are derived from field and/or laboratory tests. The procedures adopted in practice are revised or improved from time to time. There are two principal reasons for the necessary changes in methods of computation:

1. The lack of high-quality data from the results of full-scale testing of piles under axial loading. Various procedures are often used in tests reported in the technical literature, and the failure to use a recognized method leads to difficulty in evaluating results. Also, many techniques are used to obtain properties of in situ soil, and the results of soil tests often cannot be interpreted comparably. Furthermore, in only a few instances have measurements been made, using the necessary instrumentation along the length of a pile, that reveal the detailed manner in which the foundation interacts with the supporting soil.
2. The interaction between a pile and the supporting soils is complex. The soil is altered by pile installation, for example, and there are many other important factors that influence the response of a pile under axial loading. The reader is urged to read the *Proceedings, Workshop on Effects of Piles on Soil Properties,* U.S. Army Corps of Engineers, Waterways Experiment Station, Vicksburg, MS, August 1995.

Two kinds of computations are required for the analysis of pile capacity under axial loads: the computation of the ultimate axial capacity of piles under short-term loading and the computation of curves showing axial load versus settlement. More than one method is presented for obtaining axial capacity to reflect current practice among geotechnical engineers. The user may be somewhat confused because the methods produce differing results. However, the differences should not be so great as to cause concern. The reader is urged to study the basis of each analytical method in order to decide which one to use for a particular project.

In keeping with the theme of this book, soil–structure interaction, the reader is urged to use the material presented in Chapter 13 on the computation of load-settlement curves. Such a curve is shown in Figure 10.2, where the ''plunging load'' is the axial capacity. The value of the load-settlement curve, modified as necessary for long-term loading, is evident to the designers of various structures. Not only will such a curve provide a basis for the response of groups of piles, but it can also be used to determine the interaction between the foundation and the superstructure.

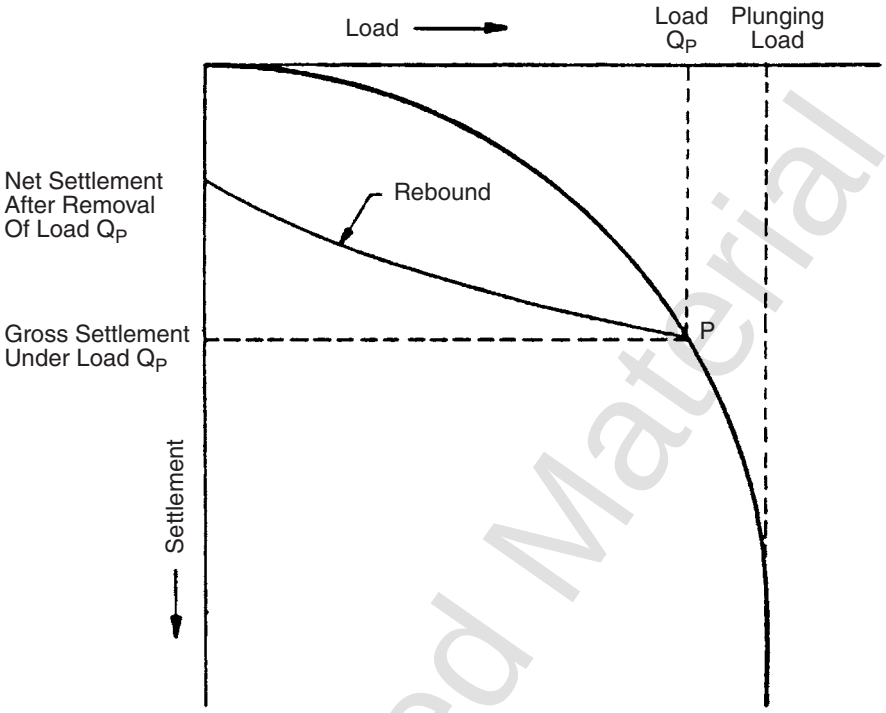

Figure 10.2 Typical load-settlement curve.

The engineer's confidence in computing the axial capacity of a pile and the load-settlement curve can be greatly enhanced by the results of field tests of piles under axial load in soils that exist at the site and installed with methods to be used in production. If there is no information in the technical literature, the engineer may be able to show that such tests, with piles of the size and penetration to be used in production, are cost effective and will greatly benefit to the proposed project.

Referring to Figure 10.2, if the load has a value of Q_p, shown by point P on the load-settlement curve, the gross settlement is indicated by the horizontal dashed line. If the load is released, some rebound will occur, as shown in the figure, with the net settlement shown for the load at zero.

10.2 METHODS OF COMPUTATION

10.2.1 Behavior of Axially Loaded Piles

The pile stiffness for axial loading in general is represented by the load-versus-settlement curve at the pile head. Some analytical methods are based

on the theory of elasticity, specifically the Mindlin equation, and solutions have been proposed by D'Appolonia and Romualdi (1963), Thurman and D'Appolonia (1965), Poulos and Davis (1968), Poulos and Mattes (1969), Mattes and Poulos (1969), and Poulos and Davis (1980). The elasticity method presents the possibility of solving for the behavior of a group of closely spaced piles under axial loadings, (Poulos, 1968; Poulos and Davis, 1980), but the weakness of the approach is that the actual ground conditions are rarely satisfied by the assumptions that must be made for E and v, the modulus of elasticity and Poisson's ratio, respectively.

A second method for obtaining the response of a single pile to axial loading represents the soil with a set of nonlinear mechanisms. The method was first used by Seed and Reese (1957); other studies are reported by Coyle and Reese (1966), Coyle and Sulaiman (1967), and Kraft et al. (1981). The method is known as the *t-z method.* A model for it is shown in Figure 10.3. Figure 10.3a shows the free body of a pile in equilibrium where the applied load Q is balanced by a tip load Q_b plus side loads Q_s. As shown in Figure 10.3c, the pile is replaced by an elastic spring and the soil is replaced by a set of nonlinear mechanisms along the pile and at the pile tip (Figure 10.3d).

The nonlinear characteristics of a hypothetical set of mechanisms, representing the response of the soil, are shown in Figure 10.3c. With regard to

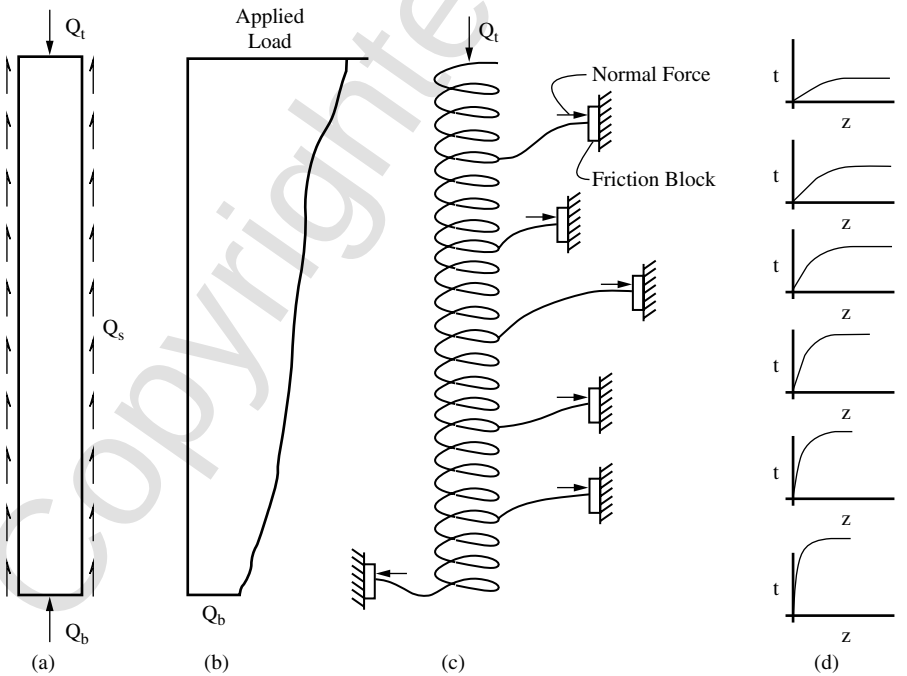

Figure 10.3 Model of an axially loaded pile.

side resistance, the ordinate t of the curves is load transfer and the abscissa z is shaft movement. The corresponding parameters for load transfer in end resistance are q and w_b. No load is transferred from pile to soil unless there is a relative movement between them. The movement is dependent on the applied load, on the position along the pile, on the stress-strain characteristics of the pile material, and on the load transfer curves.

Methods based on elasticity, while having limited applicability, satisfy the continuum effect, in contrast to the model shown in Figure 10.3, which employs the Winkler concept. That is to say, the nonlinear curves shown in Figure 10.3 are independent, while if the continuum is satisfied, all of the curves are mutually dependent. However, the recommendations for load-transfer curves are strongly based on results from full-scale loading tests where the continuum was satisfied. Further, the method has been applied with good success in the analysis of a number of field tests (Coyle and Reese, 1966; Coyle and Sulaiman, 1967), with the result that recommendations have been made for predicting the family of curves shown in Figure 10.3d.

10.2.2 Geotechnical Capacity of Axially Loaded Piles

The geotechnical capacity of an axially loaded pile is defined as the ultimate soil resistance at the point where the pile either plunges down into the ground without any further increase in load or the displacement at the pile head is too great for the superstructures. The use of static equations to compute the geotechnical capacity of piles is well established, and numerous procedures have been suggested. The first method introduced here is presented by the American Petroleum Institute (API) in their manual on recommended practice. The API procedures (see Section 10.3) have been adopted by a number of organizations. Thus, this method has some official recognition. The API procedures for clay are based essentially on the use of undrained shear strength and, of course, are largely empirical. The API procedure for sand is also strongly empirical, but effective-stress techniques are employed because no excess pore water pressures are assumed.

Three other methods, also presented here, are the method recommended by the U.S. Federal Highway Administration (FHWA), the method recommended by the U.S. Army Corps of Engineers, and the so-called Lambda method (Kraft et al., 1981). An earlier version of the Lambda method was published in 1972 (Vijayvergiya and Focht). It has been used in offshore practice because the influence of effective stresses is considered in computing skin-friction resistance.

The reader is urged to utilize all of the methods that apply to a particular soil profile. Furthermore, multiple computations should be made in which the soil parameters are varied through a range that reflects, as well as possible, the upper-bound and lower-bound values of the significant variables.

The performance of field-loading tests is strongly recommended. As noted earlier, the soil profile at a particular site can be ''calibrated'' by such field

tests so that a method of computation can be used with more confidence. The construction procedures used for the test pile and those used for the production piles should be as nearly alike as possible.

Skin Friction and Tapered Piles If tapered piles are used, only the FHWA method has the option of taking into account the taper angle for computing skin friction. All the other methods simply use the straight section for computing skin friction. Field-loading tests are strongly recommended for tapered piles because limited field test results are reported in the technical literature and there are some uncertainties about tapered piles in layered soils.

In some cases, it may be desirable to discount completely the resistance in skin friction over a portion of the pile at the ground surface—for example, if lateral deflection is such that clay is molded away from the pile. To obtain the capacity of a pile in tension, the resistance in skin friction (side resistance) may be employed. Some methods provide specific recommendations for reduction of skin friction in tension. If no reduction factor is employed in the computation, a factor of safety must be applied to the loading.

If scour close to the pile is anticipated, allowance can be made by using zeros for the shear strength of clay and for the angle of internal friction of sand in the region where scour is expected. Other values should remain unchanged so that the overburden stress reflects the position of the original ground surface.

End Bearing End bearing is computed by using the weighted average of soil properties over a distance of two diameters below the tip of the pile. In using the results of such computations, however, the designer should employ judgment in those cases where the total capacity in compression shows a sharp decrease with depth.

Soil Plug If an open pipe is used as a pile, analysis may show that a plug of soil will be forced up the inside of the pile as the pile is driven. Therefore, the end-bearing capacity of the pile is computed by adding resistance in skin friction along the inner surface plus the end bearing of the material area only. In computing resistance in skin friction along the inner surface of the pile, only the area of the thick section (driving shoe) at the end of the pile will be considered. The load from the plug is compared to the load from end bearing over the full area of the base, and the smaller of the two values is used.

The length of the end section of the pile and the internal diameter of that section are important parameters to allow the designer to make appropriate decisions concerning the development of a plug in the pile as it is driven. The remolded strength may be used to compute the internal resistance to account for the fact that the internal plug is highly disturbed as it enters the pile. If there is a length of pipe at the end of the pile with a significantly greater thickness than the pipe above, the designer may decide that only that thicker section will resist the skin friction as the plug moves up.

The designer can also change the computation of the resistance from the plug by selecting the value of the remolded shear strength of the clay that is inside the end section. The same line of reasoning holds for a pile driven into sand, except that the unit skin friction for the interior of the pile is computed the same way as the unit skin friction for the exterior of the pile.

10.3 BASIC EQUATION FOR COMPUTING THE ULTIMATE GEOTECHNICAL CAPACITY OF A SINGLE PILE

The ultimate bearing capacities are computed by use of the following equation:

$$Q_d = Q_f + Q_p = fA_s + qA_p \tag{10.1}$$

where

Q_f = total skin-friction resistance, lb (kN),
Q_p = total end bearing, lb (kN),
f = unit load transfer in skin friction (normally varies with depth), lb/ft^2 (kPa),
q = unit load transfer in end bearing (normally varies with depth), lb/ft^2 (kPa),
A_p = gross end area of the pile, ft^2 (m^2), and
A_s = side surface area of the pile, ft^2 (m^2).

Equation 10.1 is used increment by increment as the pile is assumed to penetrate the ground.

While Eq. 10.1 is generally accepted, there is no general agreement on the methods of obtaining f and q. As noted earlier, the engineer is urged to use several recommendations in the literature and use judgment in making a final design. Alternatively, a special study can be made for a specific site.

10.3.1 API Methods

The API has been active in addressing problems related to the design of fixed offshore platforms. Recommendations have been presented in a document, entitled ''API Recommended Practice for Planning, Designing, and Constructing Fixed Offshore Platforms,'' Report RP-2A. Two methods were given in RP-2A in 1986 for computing the side resistance (skin friction) in cohesive soils, Method 1 and Method 2. Method 1 was recommended for normally consolidated, highly plastic clays and Method 2 for all other types of clay. In RP-2A in1987, Method 1 and Method 2 were combined into a revised method. The revised method was included in RP-2A of 1993. The following sections

will summarize Methods 1 and 2 and the revised method of 1987. The revised method has been widely used in the offshore industry.

Skin Friction in Cohesive Soil

API Method 1. The following brief statement from API RP2A (1986) presents Method 1:

> For highly plastic clays such as found in the Gulf of Mexico f may be equal to c for under-consolidated and normally-consolidated clays. For overconsolidated clays f should not exceed 1/2 ton per square foot (48 kPa) for shallow penetrations or c equivalent to normally consolidated clay for deeper penetrations, whichever is greater. [Note: c is shown as c_n in the presentation that follows.]

The detailed explanation of the application of Method 1 follows.

$$Q_f = fA_s \tag{10.2}$$

where

Q_f = axial load capacity in skin friction,
f = unit skin friction resistance (adhesion), and
A_s = side surface area of pile.

The above equation may be written more properly as

$$Q_f = \int_0^L f_x dA_s \tag{10.3}$$

where

L = penetration of pile below ground surface, and
f_x = unit resistance in clay at depth x, measured from ground surface.

The API provision is for highly plastic clay, such as that found in the Gulf of Mexico, and the method of obtaining f_x are shown in Figure 10.4.
The step-by-step computation procedure is:

1. Construct a diagram showing undrained shear strength as a function of depth. API suggests the use of unconfined compression or miniature vane tests, and judgment should be employed in regard to the use of other data.

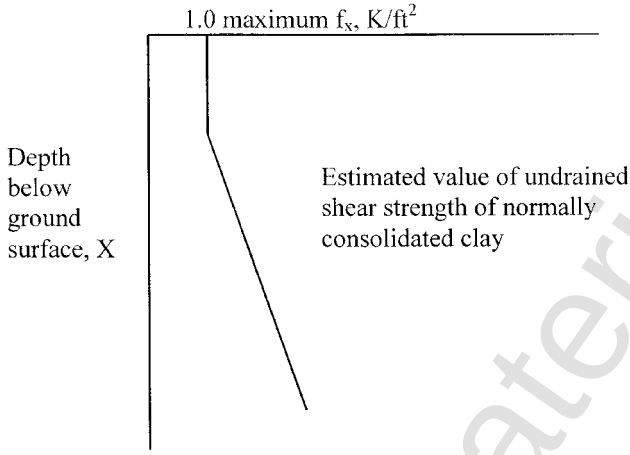

Figure 10.4 Method of obtaining f_x recommended by API RP2A (1986).

2. Construct a diagram showing the maximum f_x, as shown in Figure 10.4. The estimated value of the shear strength of normally consolidated clay may be obtained from the following expression:

$$c_n/\overline{p} = k_c = f\ (\text{PI}) \tag{10.4}$$

where

c_n = undrained shear strength of normally consolidated clay,
$\overline{p}$ = effective stress = γx,
γ = effective unit weight of soil, and
k_c = constant.

The constant k_c has been shown by Skempton and others to be a function of the plasticity index, PI. Some engineers suggest that k_c should be taken as 0.25 for Gulf of Mexico soils based on their experience. The unit weight of the soil, either total or submerged, depending on the location of the water table, should be obtained from a study of data from the soil borings for the site.

3. Select a pile of a given geometry.
4. Select an incremental length of the pile, extending from the ground surface to some depth. The length to be used is selected on the basis of the variations in the diagrams prepared in Steps 1 and 2.
5. For the incremental depth being considered in Step 4, obtain a value of the average shear strength from the diagram prepared in Step 1.

6. Compare the value obtained in Step 5 with the value of $(f_x)_{max}$ for the same depth obtained from the diagram prepared in Step 2. The smaller of the values is to be used in computing the load capacity of the pile.
7. Use the value of f_x obtained in Step 6 with the appropriate surface area of the side of the pile to compute the load capacity of the first increment. Equation 10.2, appropriately modified, can be used.
8. Select the second increment of pile penetration, with the top of the second increment being the bottom of the first increment.
9. Repeat Steps 5 through 7.
10. The loads obtained for each of the two increments can be added to obtain the total axial loading capacity of the pile in skin friction for the two increments.
11. Select other increments until the total length of the pile is taken into account.

API Method 2. The following brief statement from API RP2A (1986) presents Method 2:

> For other types of clay, f should be taken equal to c for c less or equal to 1/4 ton per square foot (24 kPa). For c in excess of 1/4 ton per square foot (24 kPa) but less than or equal to 3/4 ton per square foot (72 kPa) the ratio of f to c should decrease linearly from unity at c equal to 1/4 ton per square foot (24 kPa) to 1/2 at c equal to 3/4 ton per square foot (72 kPa). For c in excess of 3/4 ton per square foot (72 kPa), f should be taken as 1/2 of c.

The detailed explanation of the application of Method 2 follows.

$$f_x = \alpha_x c_x \tag{10.5}$$

where

α_x = coefficient that is a function of c_x, and
c_x = undrained shear strength at depth x.

The recommendation for obtaining α is shown in Figure 10.5.

Figure 10.5 states that f may be considered equal to c for undrained shear strengths of 0.5 kip per square foot or less, and equal to $0.5c$ for values of c equal to or greater than l.5 kips per square foot. For values of c between 0.5 and l.5 kips per square foot, there is a small decrease linearly, as shown.

The step-by-step computation procedure is as follows:

1. Same as Step l in Method l.
2. Same as Step 3 in Method 1.
3. Select an incremental length of pile (see Step 4 in Method l).

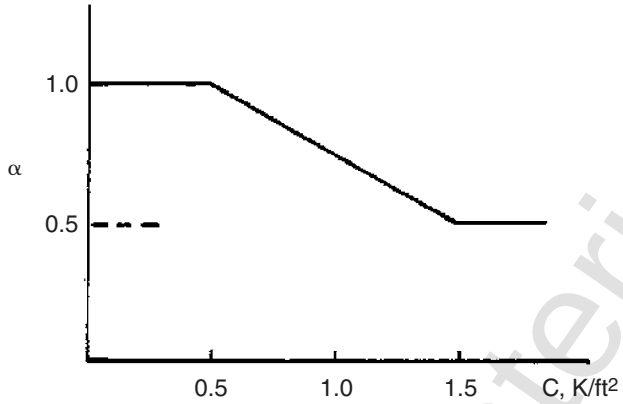

Figure 10.5 The α-value recommended by API RP2A (1986).

4. Obtain a value of c_x for the incremental length from the diagram prepared in Step l.
5. Enter Figure 10.5 with value of c_x obtained in Step 4 and obtain α_x.
6. Compute the unit skin friction resistance (unit load transfer) f_x using Eq. 10.5.
7. Compute the load capacity of the first incremental length of the pile by using Eq. 10.2 as appropriately modified.
8. Select a second increment and repeat Steps 4 through 7.
9. Add the load computed for the first two increments.
10. Select other increments of length until the length of the pile is taken into account.

Revised API Method (1987). API RP2A has proposed a revised equation for the coefficient α. The factor, α, recommended by API can be computed by two equations:

$$\alpha = 0.5\psi^{-0.5} \quad \text{if } \psi \leq 1.0$$
$$\alpha = 0.5\psi^{-0.25} \quad \text{if } \psi > 1.0 \tag{10.6}$$

with the constraint that $\alpha \leq 1.0$

where

$\psi = c/\overline{p}$ for the depth of interest,
$\overline{p}$ = effective overburden pressure, and
c = undrained shear strength of soil.

Figure 10.6 presents a comparison between α-factors calculated from 1986 and 1987 recommendations. The comparison can be made only for a specific depth because the overburden stress will change with depth; hence, for a given value of c, the value of $c/\overline{p}$ will change. The comparisons shown in Figure 10.6 are for depth where $\overline{p}$ is 0.5, 1.0, and 2.0 T/ft^2. Careful study of Figure 10.6 indicates that for normally consolidated clay, where $c/\overline{p}$ is equal approximately to 0.25, the revised method yields higher values of α than does Method 2. The revised method yields higher values of α at the depth where $\overline{p}$ is equal to 2.0 T/ft^2 (80 to 100 ft) except for heavily overconsolidated clay. The revised method yields lower values of α where $\overline{p}$ is equal to 0.5 T/ft^2 (20 to 25 ft) than does Method 2.

The step-by-step computation procedure is identical to that for Method 2 except that Eq. 10.6 is used in Step 5 instead of Figure 10.5.

End Bearing in Cohesive Soil The recommendations of API RP2A (1987) for end bearing in clay are brief: "For piles end bearing in clay, q in lb/ft^2 (kPa) should be equal to $9c$. If the strength profile below the pile tip is not uniform, then the c utilized should reflect appropriate adjustment." This recommendation is consistent with that of many other investigators.

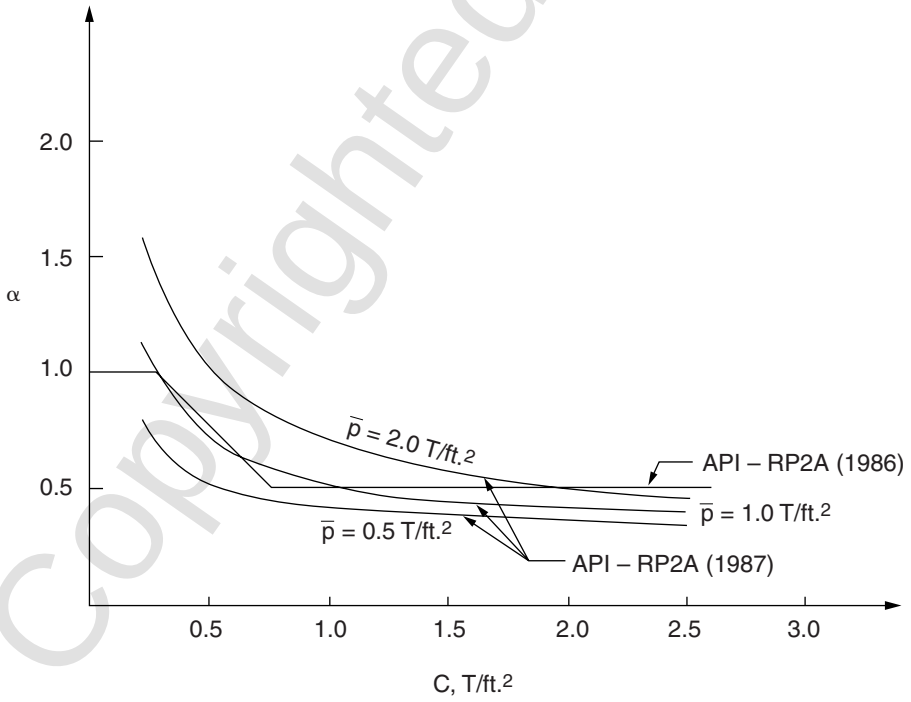

Figure 10.6 Comparison between α-factors calculated from 1986 and 1987 recommendations.

The API recommendation in equation form is as follows, along with a suggestion for modifying the value of c:

$$Q_p = qA_p \tag{10.7}$$

$$q = 9c \tag{10.8}$$

where

Q_p = axial load capacity in end bearing,
q = unit end-bearing resistance,
c = undrained shear strength at the tip of the pile, usually taken as the average over a distance of two diameters below the tip of the pile, and
A_p = cross-sectional area of the tip of the pile.

Skin Friction in Cohesionless Soil Experimental results for driven piles in sands show considerable scatter for values of skin friction and end bearing. The scatter is likely due to the influence of installation methods on soil properties and the state of stress. The following recommendations for computing unit values of skin friction and end bearing for piles in sand are consistent with the state of the practice; however, the user should use such values with caution. Pile-load tests are recommended if feasible.

The API RP2A (1987) recommendations for side resistance for pipe piles in cohesionless soil (sand) are given in the following sections.

$$f = K\overline{p}_o \tan \delta \tag{10.9}$$

where

K = coefficient of lateral earth (ratio of horizontal to vertical normal effective stress),
$\overline{p}_o$ = effective overburden pressure at the point in question, and
δ = friction angle between the soil and the pile wall.

A K value of 0.8 was recommended for open-ended pipe piles, which are driven unplugged, for loadings in both tension and compression. A K value of 1.0 was recommended for full-displacement piles. In the absence of data on δ, Table 10.1 was recommended as a guideline only for siliceous soil.

Equation 10.9 implies that the value of f increases without limit; however, Table 10.1 presents guidelines for limiting values.

End Bearing in Cohesionless Soil For end bearing in cohesionless soils, API recommends the following equation:

TABLE 10.1 Guideline for Side Friction in Siliceous Soil

Soil	δ, degrees	Limiting f, kips/ft^2 (kPa)
Very loose to medium, sand to silt	15	1.0 (47.8)
Loose to dense, sand to silt	20	1.4 (67.0)
Medium to dense, sand to sand-silt	25	1.7 (83.1)
Dense to very dense, sand to sand-silt	30	2.0 (95.5)
Dense to very dense, gravel to sand	35	2.4 (1110.8)

$$q = \overline{p}_0 N_q \tag{10.10}$$

where

$\overline{p}_0$ = effective overburden pressure at pile tip, and
N_q = bearing capacity factor.

Table 10.2 is recommended as a guideline only for siliceous soil.

The API publication points out that many soils do not fit the description of those in the tables and that the design parameters are not suitable for such soils. Examples are loose silts, soils containing large amounts of mica or volcanic grains, and calcareous sands. These latter soils are known to have substantially lower design parameters.

Drilled and grouted piles may have higher capacities than driven piles in calcareous soils.

10.3.2 Revised Lambda Method

Vijayvergiya and Focht (1972) proposed Eq. 10.11 for computing the skin-friction resistance:

$$Q_f = \lambda(p_m + 2c_m)A_s \tag{10.11}$$

TABLE 10.2 Guideline for Tip Resistance in Siliceous Soil

Soil	N_q	Limiting q, kips/ft^2 (MPa)
Very loose to medium, sand-silt	8	40 (1.9)
Loose to dense, sand to silt	12	60 (2.9)
Medium to dense, sand to sand-silt	20	100 (10.8)
Dense to very dense sand to sand-silt	40	200 (9.6)
Dense to very dense, gravel to sand	50	250 (12.0)

where

λ = a coefficient that is a function of pile penetration,
A_s = surface contact area,
p_m = mean vertical effective stress between the ground surface and the pile tip, and
c_m = mean undrained shear strength along the pile.

A curve, giving λ as a function of pile penetration, was introduced in 1972. Kraft et al. (1981) made a further study of data and revised the method of obtaining λ. The following equations were employed.

For normally consolidated soils:

$$\lambda = 0.178 - 0.016 \ln \pi_3 \tag{10.12a}$$

For overconsolidated soils:

$$\lambda = 0.232 - 0.032 \ln \pi_3 \tag{10.12b}$$

where

$$\pi_3 = (\pi B f_{\max}(L_e^2)/(AEU)), \tag{10.13}$$

B = pile diameter,
$f_{\max}$ = peak skin friction (taken as the mean undrained shearing strength),
L_e = embedded pile length,
A = cross-sectional area of pile material,
E = modulus of elasticity of pile material, and
U = pile displacement needed to develop the side shear (taken as 0.1 in.).

In the absence of data consolidation, Kraft et al. considered the clay to be overconsolidated if the undrained shear strength divided by the overburden stress was equal to or larger than 0.10. The value of the lower limit of λ was taken as 0.110.

The step-by-step computation procedure is as follows:

1. Construct a diagram showing undrained shear strength as a function of depth.
2. Construct a diagram showing vertical effective stress as a function of depth.

3. Select a pile of a given geometry.
4. Select a pile penetration for computation of the axial load capacity in skin friction.
5. Use the diagram constructed in Step 1 and compute c_m.
6. Use the diagram constructed in Step 2 and compute p_m.
7. Obtain the value of λ from Eqs. 10.12 through 10.13.
8. Substitute values of λ, p_m, and c_m, along with the value of A_s, into Eq. 10.11 and compute Q_f.
9. Select a different pile penetration and repeat Steps 5 through 8 to obtain the pile capacity Q_f as a function of pile penetration.

10.3.3 U.S. Army Corps Method

Piles in Cohesionless Soil

Skin Friction. For design purposes, the skin friction of piles in sand increases linearly to an assumed critical depth (D_c) and then remains constant below that depth. The critical depth varies between 10 to 20 pile diameters or widths (B), depending on the relative density of the sand. For cylindrical piles, B is equal to the pile diameter. The critical depth is assumed as:

$D_c = 10B$ for loose sands,
$D_c = 15B$ for medium dense sands, and
$D_c = 20B$ for dense sands.

The unit skin friction acting on the pile shaft may be determined by the following equations:

$$f_s = k\sigma'_v \tan \delta$$

$$\sigma'_v = \gamma' D \quad \text{for} \quad D < D_c$$

$$\sigma'_v = \gamma' D_c \quad \text{for} \quad D \geq D_c$$

$$Q_s = f_s A \tag{10.14}$$

where

K = lateral earth pressure coefficient (K_c for compression piles and K_t for tension piles),
σ'_v = effective overburden pressure,
δ = angle of friction between the soil and the pile,

γ' = effective unit weight of soil, and
D = depth along the pile at which the effective overburden pressure is calculated.

Values of δ are given in Table 10.3.

Values of K for piles in compression (K_c) and piles in tension (K_t) are given in Table 10.4. Tables 10.3 and Table 10.4 present ranges of values of δ and K based upon experience in various soil deposits. These values should be selected for design based upon experience and pile load test results. The designer should not use the minimum reduction of the ϕ angle while using the upper-range K values.

For steel H-piles, A_s should be taken as the block perimeter of the pile and δ should be the average friction angle of steel against sand and sand against sand (ϕ.). Note that Table 10.4 provides general guidance to be used unless the long-term engineering practice in the area indicates otherwise. Under prediction of soil strength, parameters at load test sites have sometimes produced back-calculated values of K that exceed the values in Table 10.4. It has also been found, both theoretically and at some test sites, that the use of displacement piles produces higher values of K than does the use of nondisplacement piles. Values of K that have been used satisfactorily but with standard soil data in some locations are presented in Table 10.5.

End Bearing. For design purposes, the bearing capacity of the tip of the pile can be assumed to increase linearly to a critical depth (D_c) and then remain constant. The same critical depth relationship used for skin friction can be used for end bearing. The unit tip bearing capacity can be determined as follows:

$$q = \sigma_v' N_q \tag{10.15}$$

where

$\sigma_v' = \gamma' D$ for $D < D_c$,
$\sigma_v' = \gamma' D_c$ for $D \geq D_c$, and
N_q = bearing capacity factor.

TABLE 10.3 Values of δ

Pile Material	δ
Steel	0.67 ϕ to 0.83 ϕ
Concrete	0.90 ϕ to 1.0 ϕ
Timber	0.80 ϕ to 1.0 ϕ

TABLE 10.4 Values of *K*

Soil Type	K_c	K_t
Sand	1.00 to 2.00	0.50 to 0.70
Silt	1.00	0.50 to 0.70
Clay	1.00	0.70 to 1.00

Note: The above values do not apply to piles that are prebored, jetted, or installed with a vibratory hammer. Selection of K values at the upper end of these ranges should be based on local experience. K, δ, and N_q values back-calculated from load tests may be used.

For steel H-piles, A_t should be taken as the area included within the block perimeter. A curve to obtain the Terzaghi-Peck (1967) bearing capacity factor N_q (among values from other theories) is shown in Figure 10.7. To use the curve, one must obtain measured values of the angle of internal friction (ϕ) which represents the soil mass.

Tensile Capacity. The tensile capacity of piles in sand, which should not include the end bearing, can be calculated as follows using the K_t values for tension from Table 10.4:

$$Q_{\text{ult}} = Q_{s,\text{tension}}$$

Piles in Cohesive Soil

Skin Friction. Although called skin friction, the resistance is due to the cohesion or adhesion of the clay to the pile shaft.

$$f_s = c_a$$

$$c_a = \alpha c$$

$$Q_s = f_s A_s \tag{10.16}$$

TABLE 10.5 Common Values for Corrected *K*

	Displacement Piles		Nondisplacement Piles	
Soil Type	Compression	Tension	Compression	Tension
Sand	2.00	0.67	1.50	0.50
Silt	1.25	0.50	1.00	0.35
Clay	1.25	0.90	1.00	0.70

Note: Although these values may be commonly used in some areas, they should not be used without experience and testing to validate them.

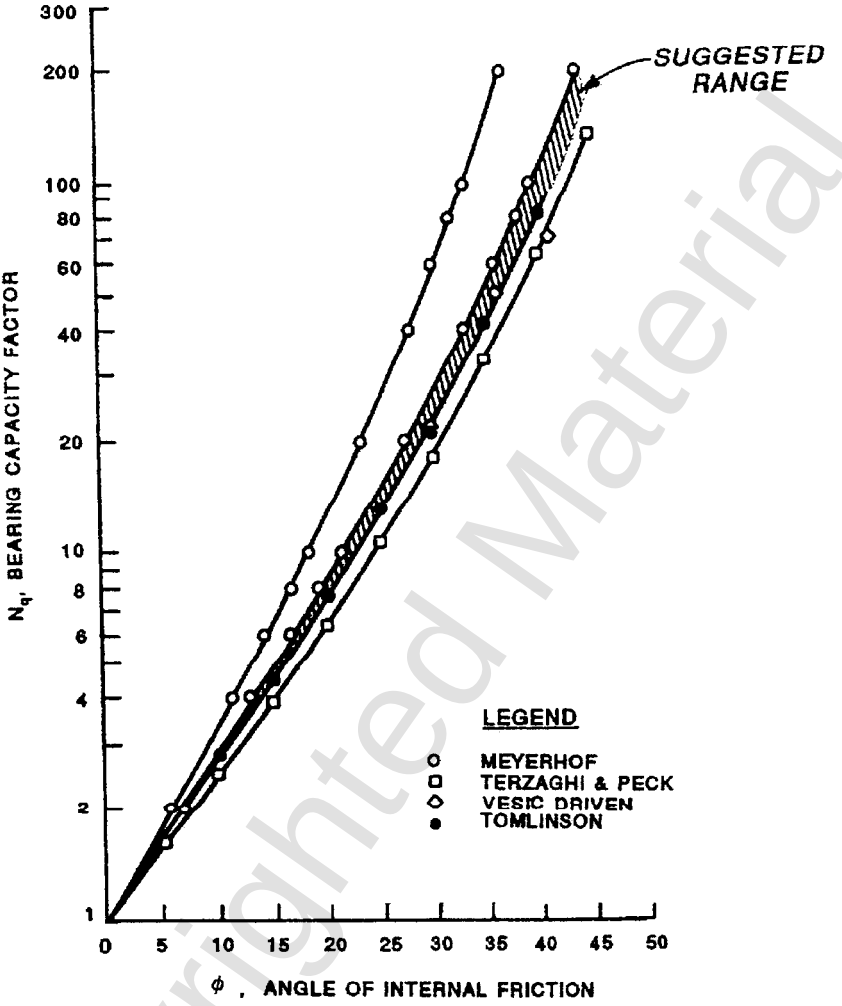

Figure 10.7 Bearing capacity factor N_q.

where

c_a = adhesion between the clay and the pile,
α = adhesion factor, and
c = undrained shear strength of the clay from a quick (Q) test.

The values of α as a function of undrained shear strength are given in Figure 10.8.

An alternative procedure developed by Semple and Rigden (1984) to obtain values of α that are especially applicable to very long piles is given in Figure 10.9, where

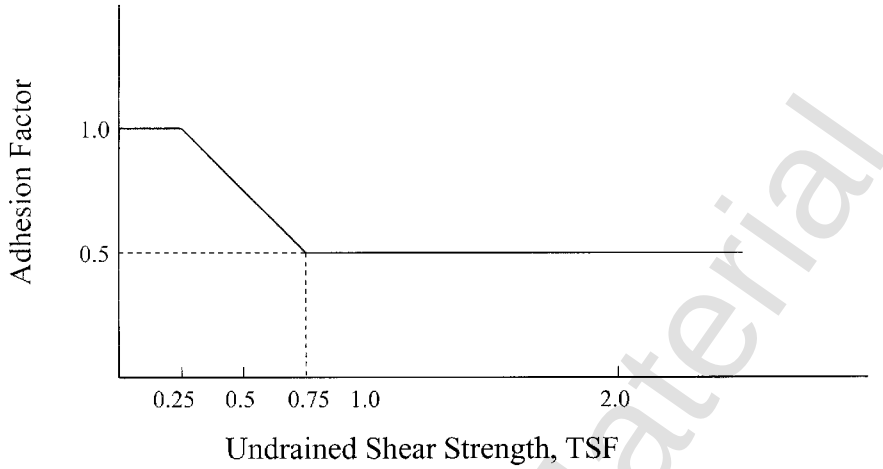

Figure 10.8 Value of α versus undrained shear strength recommended by the U.S. Army Corps method.

$$\alpha = \alpha_1 \alpha_2 \tag{10.17}$$

and

$$f_s = \alpha c \tag{10.18}$$

End Bearing. The pile unit-tip bearing capacity for piles in clay can be determined from the following equations:

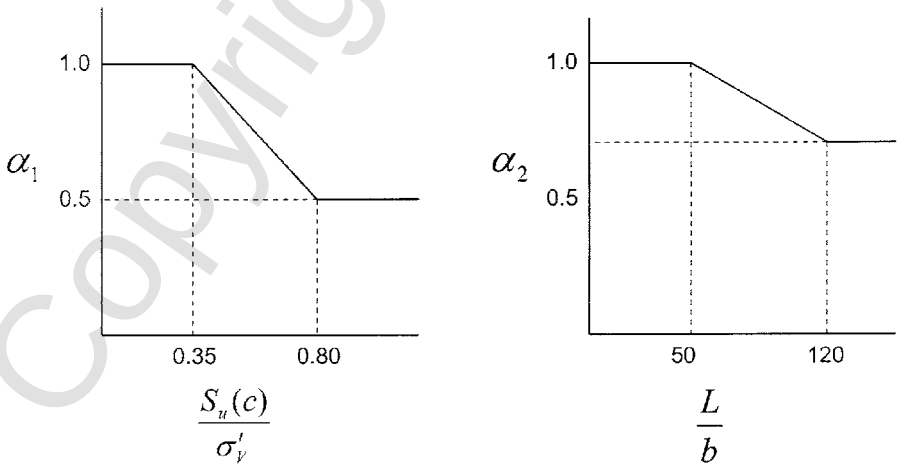

Figure 10.9 Value of α_1, α_2 applicable to very long piles.

$$q = 9c \tag{10.19}$$

$$Q_t = A_t q \tag{10.20}$$

However, the movement necessary to develop the tip resistance of piles in clay soils may be several times larger than that required to develop the skin friction resistance.

Compressive Capacity. By combining the skin friction and the top bearing capacity, the ultimate compression capacity may be found:

$$Q_{\text{ult}} = Q_s + Q_t \tag{10.21}$$

Tensile Capacity. The tensile capacity of piles in clay may be calculated as

$$Q_{\text{ult}} = Q_s \tag{10.22}$$

S-Case Shear Strength. The pile capacity in normally consolidated clays (cohesive soils) should also be computed in the long-term S shear strength case. That is, the engineer should develop an S-Case shear strength trend as discussed previously and proceed as if the soil is drained. The computational method is identical to that for piles in granular soils, and to present the computational methodology would be redundant. Note, however, that the shear strengths in clays in the S-Case are assumed to be $\phi > 0$ and $c = 0$. Some commonly used S-Case shear strengths in alluvial soils are reported in Table 10.6.

These general data ranges are from tests on specific soils in site-specific environments and may not represent the soil in question.

10.3.4 FHWA Method

Introduction Contrary to the methods presented above, the FHWA method uses the same general equations for computing the response of a pile in both sands and clays. A single pile derives its load-carrying ability from the fric-

TABLE 10.6 S-Case Shear Strength

Soil Type		Consistency	Angle of Internal Friction
Fat clay	(CH)	Very soft	13–17
Fat clay	(CH)	Soft	17–20
Fat clay	(CH)	Medium	20–21
Fat clay	(CH)	Stiff	21–23
Silt	(ML)		25–28

Note: The designer should perform testing and select shear strengths.

tional resistance of the soil around the shaft and the bearing capacity at the pile tip:

$$Q = Q_p + Q_s \tag{10.23}$$

where

$$Q_p = A_p q_p \tag{10.24}$$

and

$$Q_s = \int_0^L f_s C_d dz \tag{10.25}$$

where

A_p = area of pile tip,
q_p = unit bearing capacity at pile tip,
f_s = ultimate skin resistance per unit area of shaft C_d,
C_d = effective perimeter of pile,
L = length of pile in contact with soil, and
z = depth coordinate.

Point Resistance The point bearing capacity can be obtained from

$$q_p = cN_c + qN_q + \frac{B}{2} N_\gamma \tag{10.26}$$

where N_c, N_q, and N_γ are dimensionless parameters that depend on the soil friction angle ϕ. The term c is the cohesion of the soil, q is the vertical stress at the pile base level, B is the pile diameter (width), and γ is the unit weight of the soil.

For end bearing in cohesive soils, Eq. 10.27 is recommended:

$$Q_p = A_p \, c \, N_c \tag{10.27}$$

Values of N_c lie between 7 and 16. A value of $N_c = 9$ is usually used.

For end bearing in cohesionless soils, the FHWA method uses the following equation:

$$Q_p = A_p \, \overline{q} \, \alpha \, N'_q \tag{10.28}$$

where

N'_q = bearing capacity factor from Figure 10.10 and
α = dimensionless factor dependent on the depth–width relationship of the pile in Figure 10.10.

Meyerhof (1976) recommends the limiting value for the tip resistance in cohesive soils as shown in Figure 10.11.

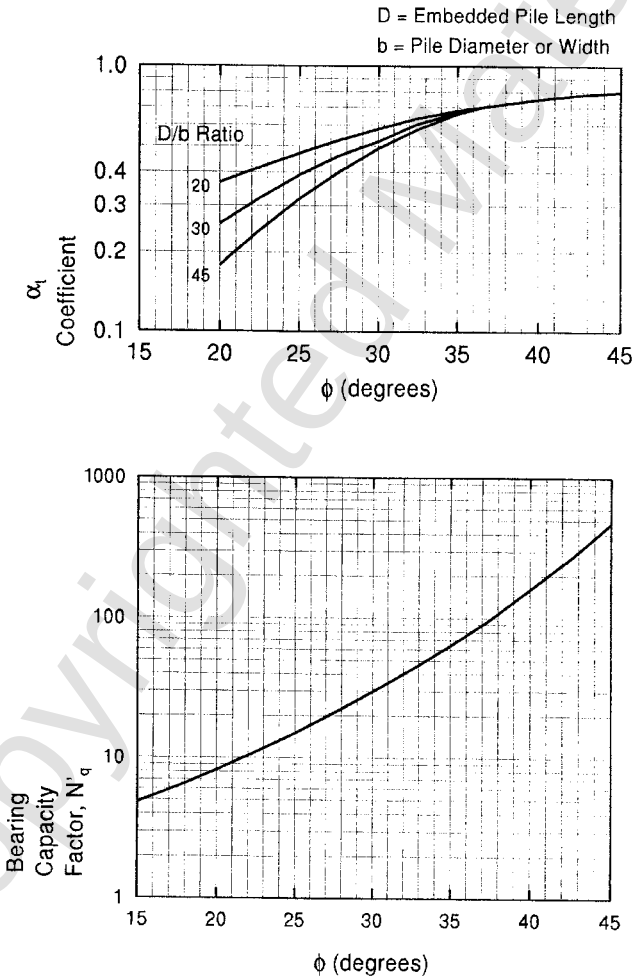

Figure 10.10 Chart for estimating the α coefficient and the bearing capacity factor N_q.

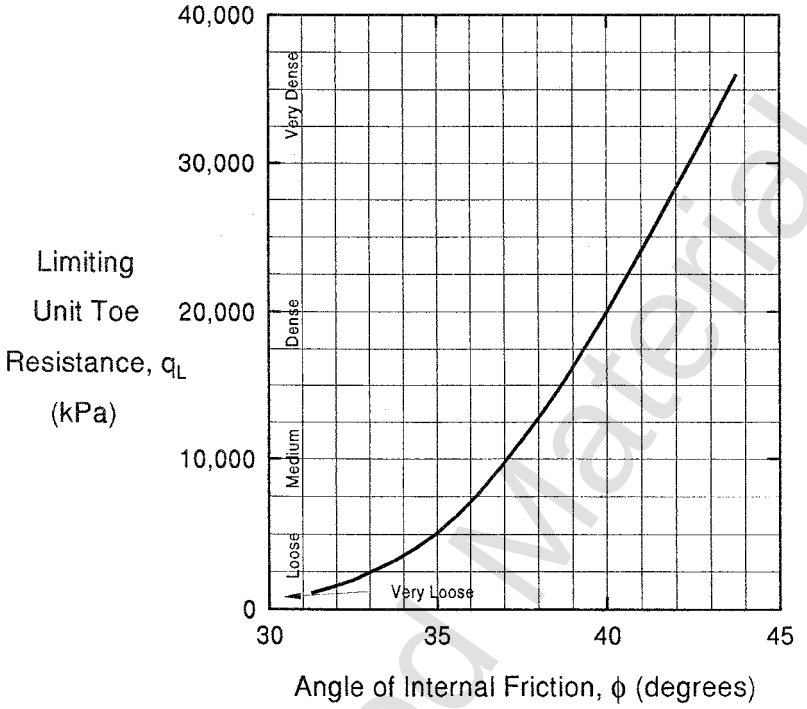

Figure 10.11 Relationship between maximum unit pile point resistance and friction angle for cohesionless soils recommended by Meyerhof (1976) (after FHWA, 1993).

Side Resistance The ultimate side resistance per unit area of shaft is calculated as follows:

$$f_s = c_a + \sigma_h \tan \delta \tag{10.29}$$

where

c_a = pile–soil adhesion,
σ_h = normal component of stress at pile–soil interface, and
δ = pile–soil friction angle.

The normal stress σ_h is related to the vertical stress σ_v as $\sigma_h = K\sigma_v$, where K is a coefficient of lateral stress. Substituting into Eq. (10.29) produces this result:

$$f_s = c_a + K\sigma_v \tan \delta \tag{10.30}$$

For cohesive soils, Eq. (10.30) reduces as follows:

$$f_s = c_a \tag{10.31}$$

where the adhesion c_a is usually related to the undrained shear strength c_u in the following way:

$$c_a = \alpha c_u \tag{10.32}$$

where α is an empirical adhesion coefficient that depends mainly upon the following factors: nature and strength of the soil, type of pile, method of installation, and time effects. Figure 10.12 presents the α-values used by the program as suggested by Tomlinson (1980).

For cohesionless soils, Eq. 10.30 reduces to

$$f_s = \overline{c}_a + K\overline{\sigma}_v \tan \delta \cong K\overline{\sigma}_v \tan \delta \tag{10.33}$$

because $\overline{c}_a$ is either zero or small compared to $K\overline{\sigma}_v \tan \delta$.

The main difficulty in applying the effective stress approach lies in having to predict the normal effective stress on the pile shaft $\overline{\sigma}_h = K\overline{\sigma}_v$.

Nordlund (1963, 1979) developed a method of calculating skin friction based on field observations and results of several pile load tests in cohesionless soils. Several pile types were used, including timber, H, pipe, monotube, and others. The method accounts for pile taper and for differences in pile materials.

Nordlund suggests the following equation for calculating the ultimate skin resistance per unit area:

$$f_s = K_\delta C_f \overline{p}_d \frac{\sin(\omega + \delta)}{\cos \omega} C_d dz \tag{10.34}$$

Combine Eq. (10.25) with Eq. (10.34) to calculate the frictional resistance of the soil around the pile shaft as follows:

$$Q_s = \int_0^L K_\delta C_f \overline{p}_d \frac{\sin(\omega + \delta)}{\cos \omega} C_d dz \tag{10.35}$$

which simplifies for nontapered piles ($\omega = 0$) as follows:

$$Q_s = \int_0^L k_\delta C_f \overline{p}_d \sin(\delta) C_d dz \tag{10.36}$$

where

Q_s = total skin friction capacity,
K_δ = coefficient of lateral stress at depth z,

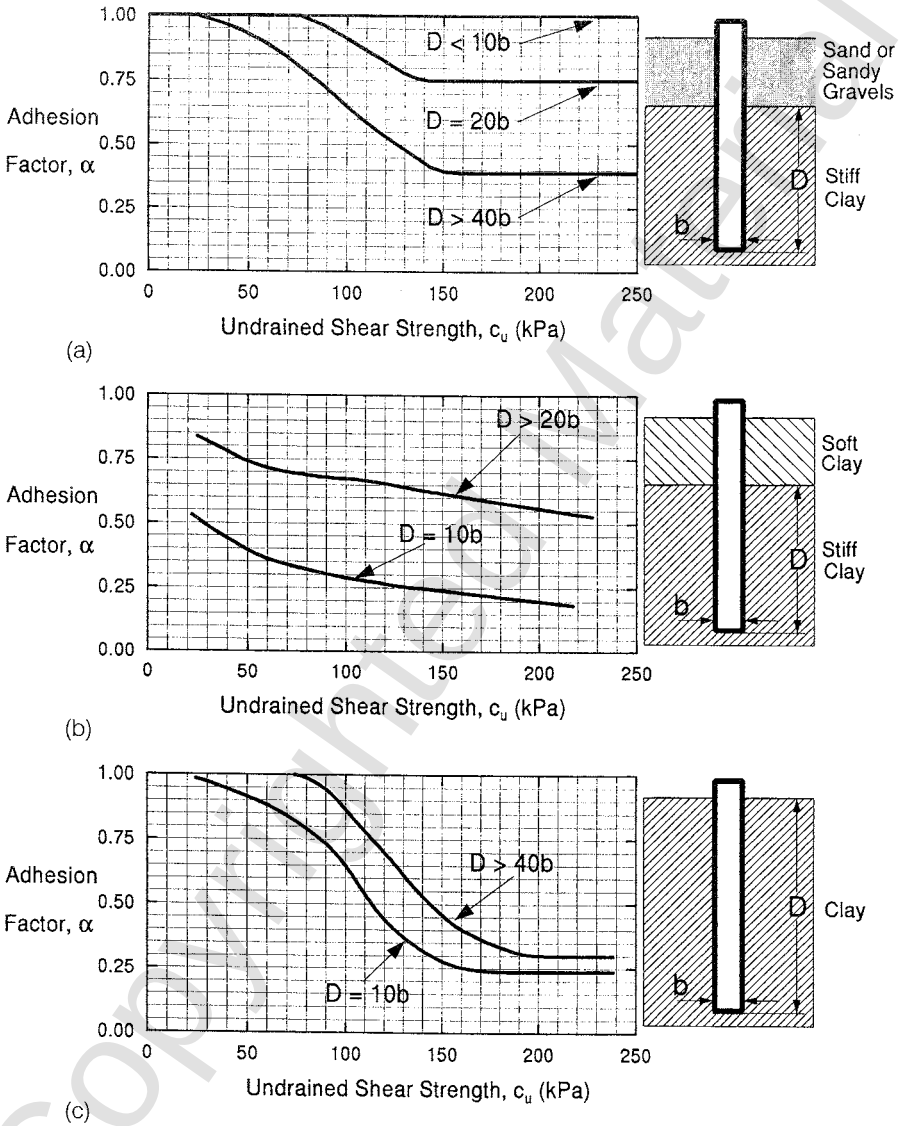

Figure 10.12 Adhesion factors for driven piles in clay recommended by Tomlinson (1980) (after FHWA, 1993).

$\bar{p}_d$ = effective overburden pressure,
ω = angle of pile taper from vertical,
δ = pile–soil friction angle,
C_d = effective pile perimeter, and
C_f = correction factor for K_δ when $\delta \neq \phi$.

To avoid numerical integration, computations are performed for pile segments within soil layers of the same effective unit weight and friction angle. Then Eq. 10.36 becomes

$$Q_s = \sum_{i=1}^{n} K_{\delta_i} C_{f_i} \bar{p}_{d_i} D_i \sin(\delta) \tag{10.37}$$

where

n = number of segments, and
D_i = thickness of single segment.

Figures 10.13 to 10.16 give values of K_δ versus ϕ with δ equal to ϕ, and Figure 10.17 gives a correction factor to be applied to K_δ when δ is not equal to ϕ.

Nordlund (1963, 1979) states that the angle of friction (δ) between the soil and the pile depends on the pile material and the displaced volume per foot during pile installation. Figure 10.18 gives δ/ϕ for different pile types and sizes.

Figure 10.19 shows the correction factor of field SPT N-values for the influence of effective overburden pressure, and Figure 10.20 shows a correlation between SPT N-values and $\tilde{\phi}$.

10.4 ANALYZING THE LOAD–SETTLEMENT RELATIONSHIP OF AN AXIALLY LOADED PILE

10.4.1 Methods of Analysis

The foundation engineer must make a number of simplifying assumptions in the design procedure for axially loaded piles. These assumptions are necessary to quantify the behavior of the pile-soil system. One of the most grossly oversimplifying assumptions in the static formula is that the ultimate bearing capacity of the soil at the tip of the pile and the ultimate skin friction along the pile shaft are mobilized simultaneously, with no regard for the displacement compatibility of these separate components. Another oversimplifying assumption is that the soil conditions existing prior to installation are still present after placement of the pile.

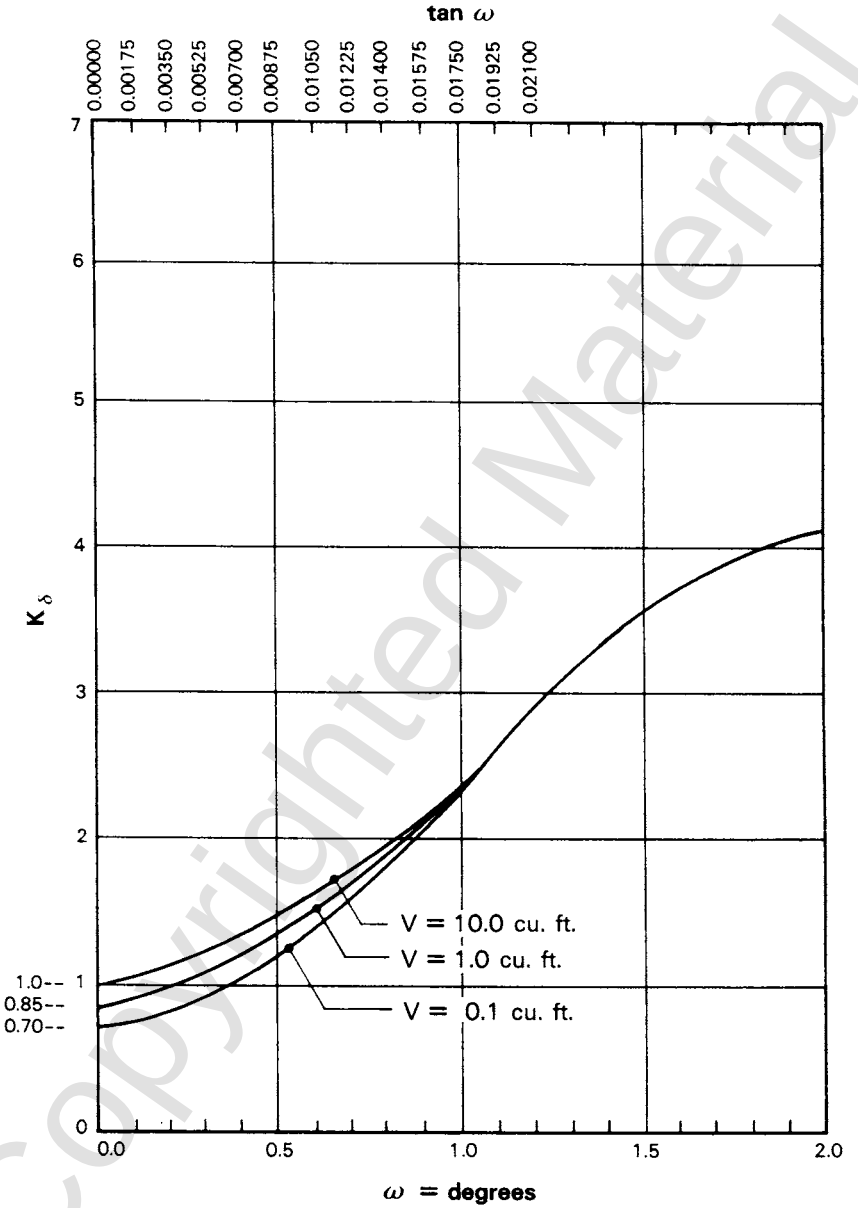

Figure 10.13 Design curves for evaluating K_δ for piles when $\phi = 25°$ recommended by Nordlund (1979) (after FHWA, 1993).

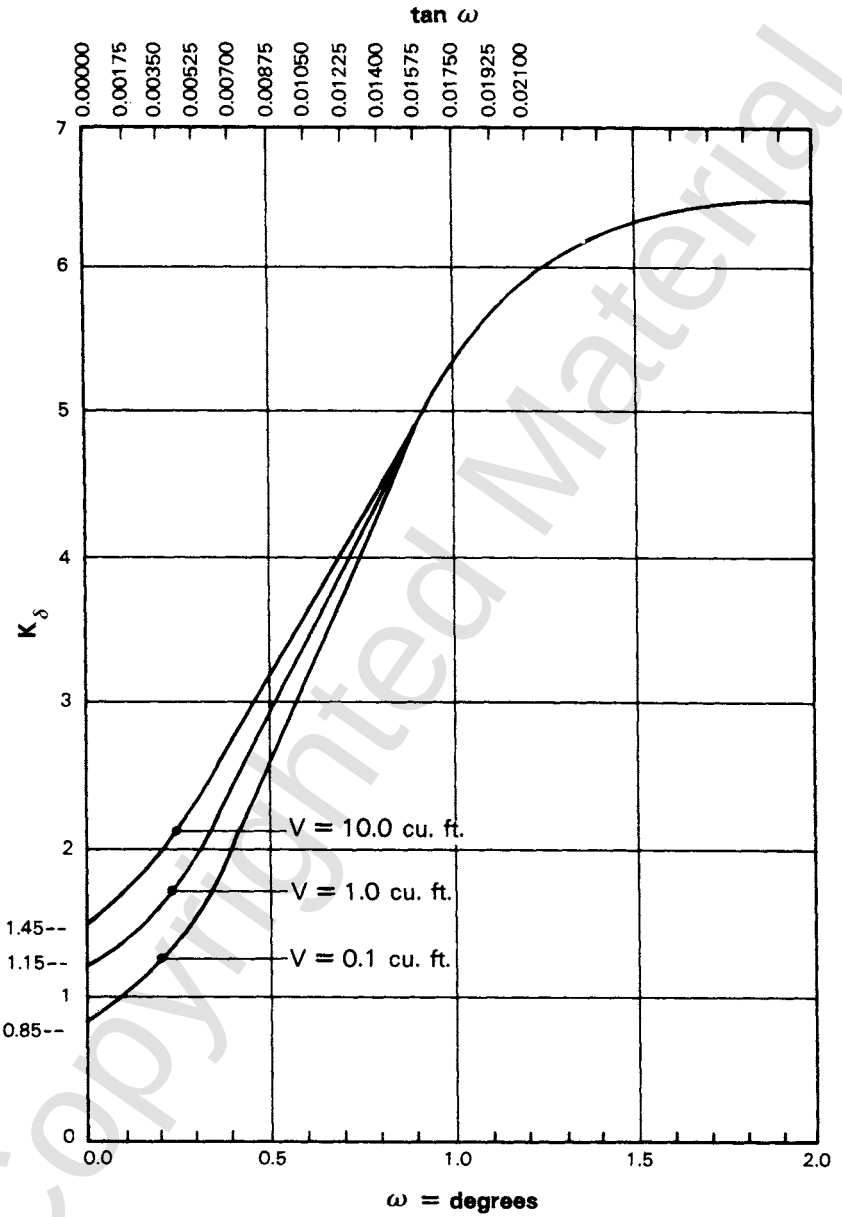

Figure 10.14 Design curves for evaluating K_δ for piles when $\phi = 30°$ recommended by Nordlund (1979) (after FHWA, 1993).

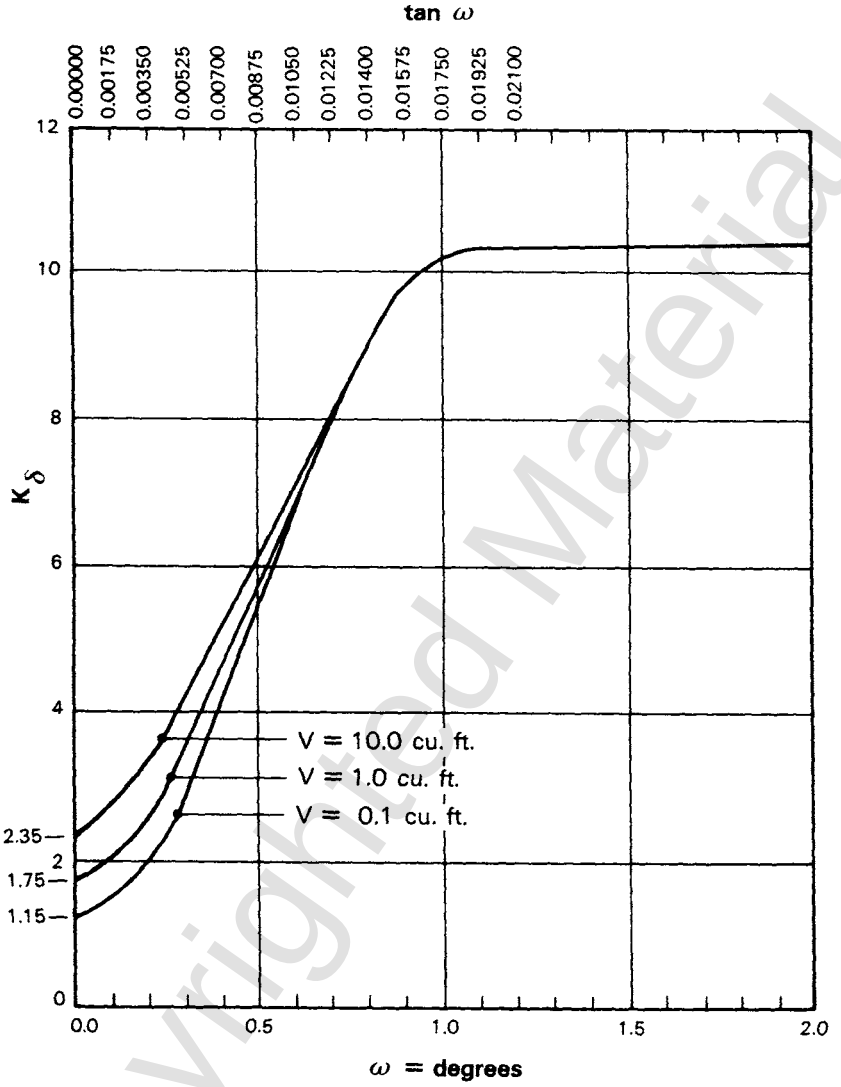

Figure 10.15 Design curves for evaluating K_δ for piles when $\phi = 35°$ recommended by Nordlund (1979) (after FHWA, 1993).

The drawback of the elasticity method lies in the basic assumptions that must be made. The actual ground condition rarely satisfies the assumption of uniform and isotropic material. In spite of the highly nonlinear stress-strain characteristics of soils, the only soil properties considered in the elasticity method are Young's modulus E and Poisson's ratio v. The use of only two constants, E and v, to represent soil characteristics is a gross oversimplification. In actual field conditions, v may be relatively constant, but E can vary through several orders of magnitude.

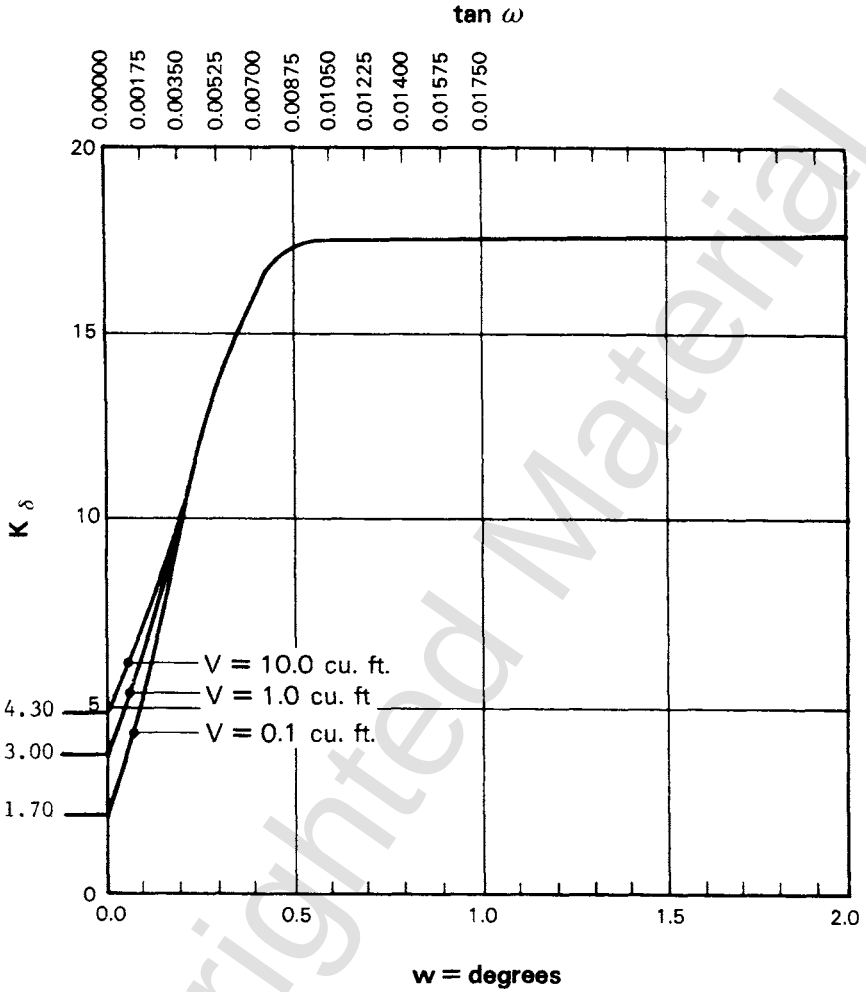

Figure 10.16 Design curves for evaluating K_δ for piles when $\phi = 40°$ recommended by Nordlund (1979) (after FHWA, 1993).

The other method used to calculate the load-versus-settlement curve for an axially loaded pile may be called the *t-z method* as presented in Section 10.2.1. Finite-difference equations are employed to achieve compatibility between the pile displacement and the load transfer along a pile and between displacement and resistance at the tip of the pile. The t-z method assumes the Winkler concept; that is, the load transfer at a certain pile section and the pile-tip resistance are independent of the pile displacement elsewhere. The close agreement between prediction and loading-test results in clays (Coyle and Reese, 1966) and the scattering of prediction for loading tests in sands (Coyle and Sulaiman, 1967) may possibly be explained by the relative sen-

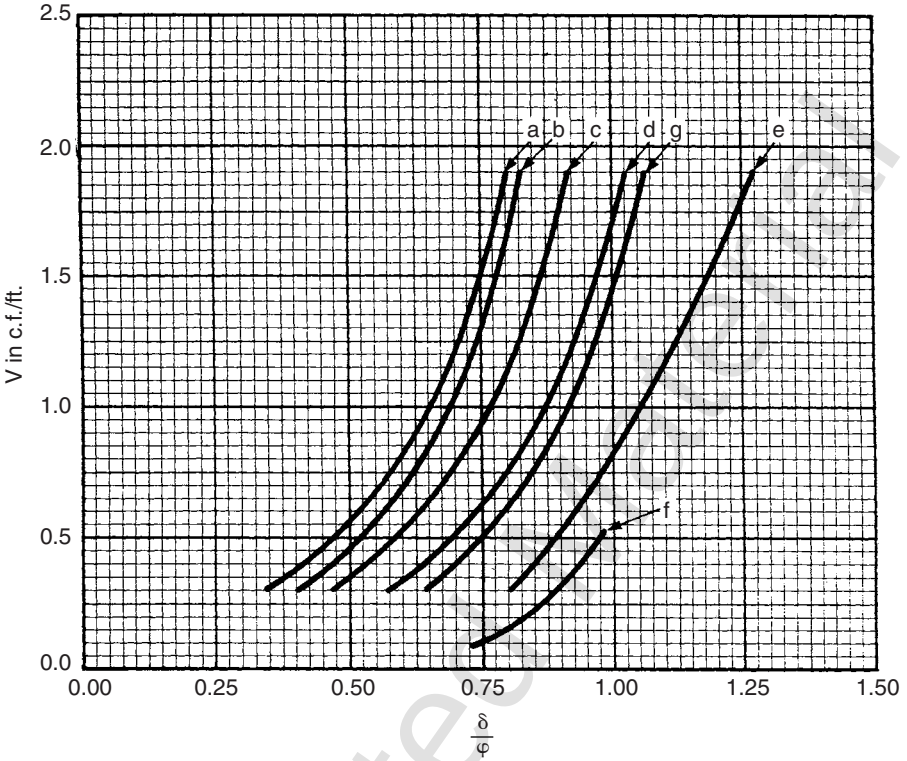

Figure 10.17 Correction factor for K_δ when δ and ϕ are not equal recommended by Nordlund (1979) (after FHWA, 1993).

sitivity of a soil to changes in patterns of stress. Admitting the deficiency in the displacement-shear-force criteria of sand, the t-z method is still a practical method because it can deal with any complex composition of soil layers with any nonlinear relationship of displacement versus shear force. Furthermore, the method can accommodate improvements in soil criteria with no modifications of the basic theory.

The fundamental problem in computing a load-settlement curve, and curves showing the distribution of axial load as a function of distance along the pile, is to select curves that show load transfer in side resistance (skin friction) as a function of pile movement at the point in question (commonly called *t-z curves*) and a curve showing end bearing as a function of movement of the pile tip (commonly called a *q-w curve*).

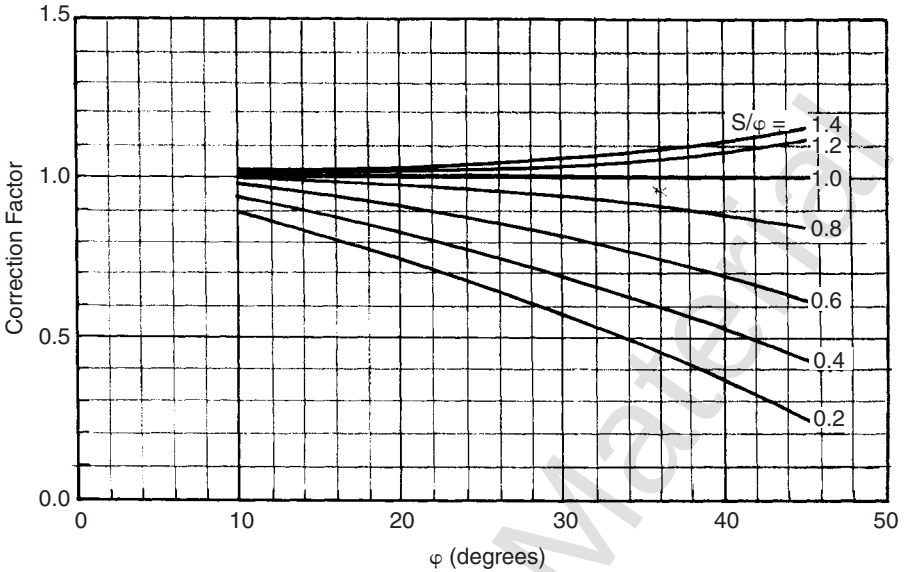

Figure 10.18 Relation δ/ϕ and pile displacement, V, for various types of piles recommended by Nordlund (1979) (after FHWA, 1993).

A computer program named APILEplus was developed based on the methods of computation presented in this chapter. The program utilizes two related codes to provide information on the behavior of driven piles under axial loading. The first code uses four different sets of recommendations for computing the axial capacity of piles as a function of depth. The second code employs *t-z* curves to compute the load versus settlement of the pile at the greatest length that is specified by the engineer. The program also has the flexibility to allow users to specify any types of values for the transfers in skin friction and end bearing as a function of depth. This feature is useful for cases when the site measurements were made from axial load tests.

10.4.2 Interpretation of Load-Settlement Curves

A typical load-settlement curve for a deep foundation was presented in Figure 10.2. The failure load of a driven pile can be interpreted in several different ways from the load settlement curves at the pile head. There is no doubt that the failure occurs when the pile plunges down into the ground without any further increase in load. However, from the point of view of the service requirement, the pile fails when its settlement reachs the stage at which unacceptable distortion might occur in the structure. The maximum allowable settlement at the top of the pile is typically specified by the designer of the structure.

The procedure recommended by Davisson (1972) for obtaining the failure load based on the load-settlement curve is widely accepted for driven piles.

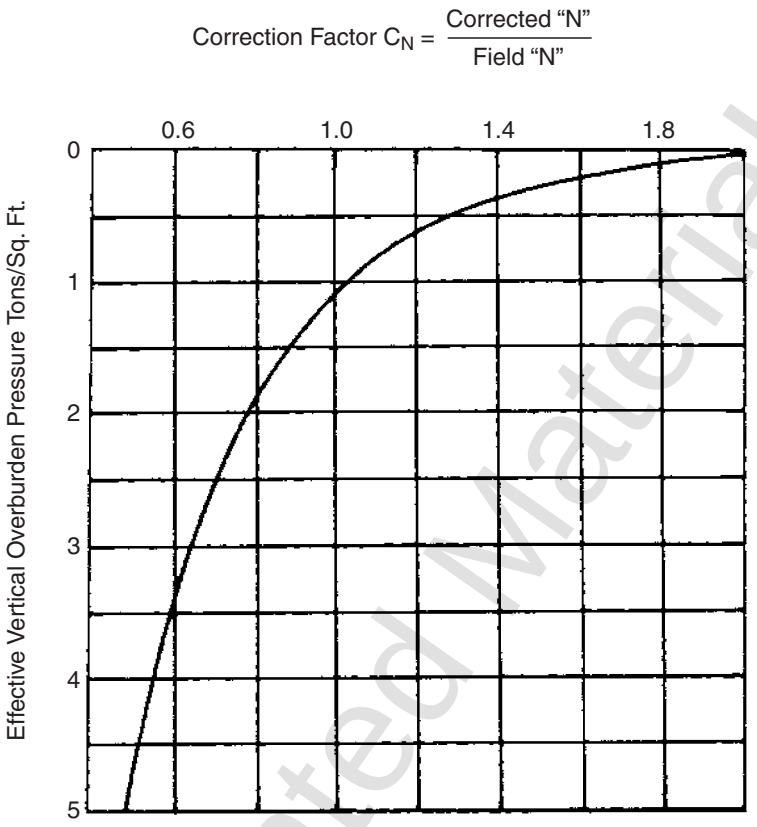

Figure 10.19 Chart for correction of *N*-values in sand for influence of effective overburden pressure (after FHWA, 1993).

Davisson's method takes into account the elastic shortening of the pile under the axial load, the required relative movement (0.15 in.) between the soil and the pile for full mobilization of side friction, and the amount of tip movement (1/120th of the pile diameter in inches) for mobilization of tip resistance. Therefore, the total movement under the failure load is as shown in Figure 10.21.

$$\Delta = (P_{ult})(L)/(AE) + 0.15 \text{ in.} + D/120 \text{ in.} \tag{10.38}$$

where

P_{ult} = failure load,
L = pile length,
A = area of pile cross section,
E = elastic modulus of pile material, and
D = pile diameter.

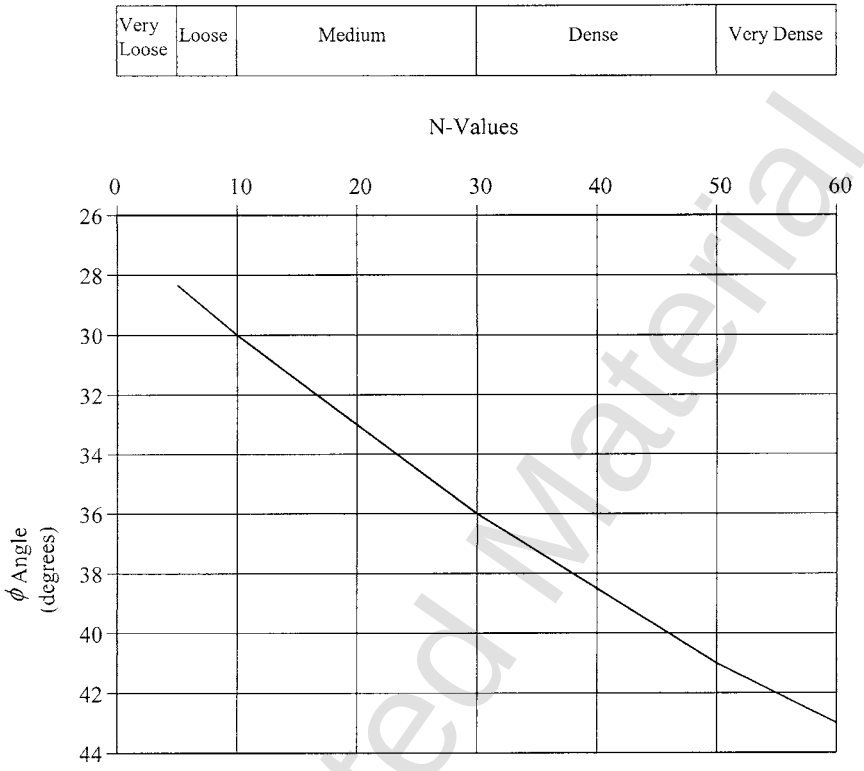

Figure 10.20 Relationship between SPT values and ϕ or relative density descriptions recommended by Peck et al. (1974) (after FHWA, 1993).

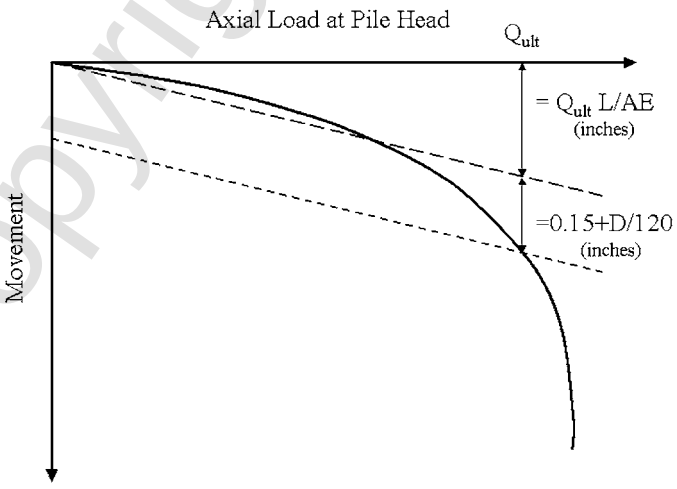

Figure 10.21 Interpretation of the load-settlement curve.

Other recommendations consider that the pile has failed when the pile head has moved 10% of the pile end diameter or a total gross settlement of 1.5 in. The definition of the failure load may involve judgment for some cases. However, the full range of the load-settlement curve at the pile head predicted by the *t-z* method is always beneficial to the designer, allowing better control of the movement of the structure components.

10.5 INVESTIGATION OF RESULTS BASED ON THE PROPOSED COMPUTATION METHOD

Minami (1983) made a study employing one set of recommendations for load-transfer curves in which the results from field-load tests of 10 piles were analyzed. The piles were tested in Japan, and the relevant data were available. Table 10.7 shows pertinent data about the various piles. The first step was to modify the soil properties as necessary to ensure that the ultimate capacity as computed was in agreement with the experiment. Then load-settlement curves were computed; Figure 10.22 shows comparisons of settlements for the 10 cases. The comparisons were made at one-half of the ultimate capacity, as found in the experiment.

Figure 10.22 shows that agreement was reasonable for this type of computation except for perhaps three cases where the predicted settlements were significantly greater that the measured ones. Some of the error may be due to experimental values such as load, settlement, pile geometry and stiffness, and soil properties. Most of the difference probably is due to the inability to predict correctly the load-transfer curves. Therefore, it is recommended that upper-bound and lower-bound solutions be developed by varying the input parameters through an appropriate range.

TABLE 10.7 Pertinent Data on the Various Piles Studied by Minami (1983)

No.	Type	Length (ft)	Outside Diameter (in.)	Soil	Experimental Load Capacity (kips)
1	SP	67.3	31.5	Sand	1058
2	SP	88.6	28.0	Clay, sand	1234
3	SP	105.0	31.5	Clay, sand	727
4	SP	67.3	31.5	Sand	1102
5	SP	137.8	31.5	Sand	661
6	PC	53.3	19.7	Clay, sand	661
7	PC	100.1	23.6	Clay, sand	881
8	CP	88.6	39.4	Sand	1432
9	PC	106.6	17.7	Clay, sand	705
10	SP	111.6	18.0	Sand	639

*Type of pile
SP = Steel pipe pile, PC = Precast concrete pile, CP = Cast-in place pile

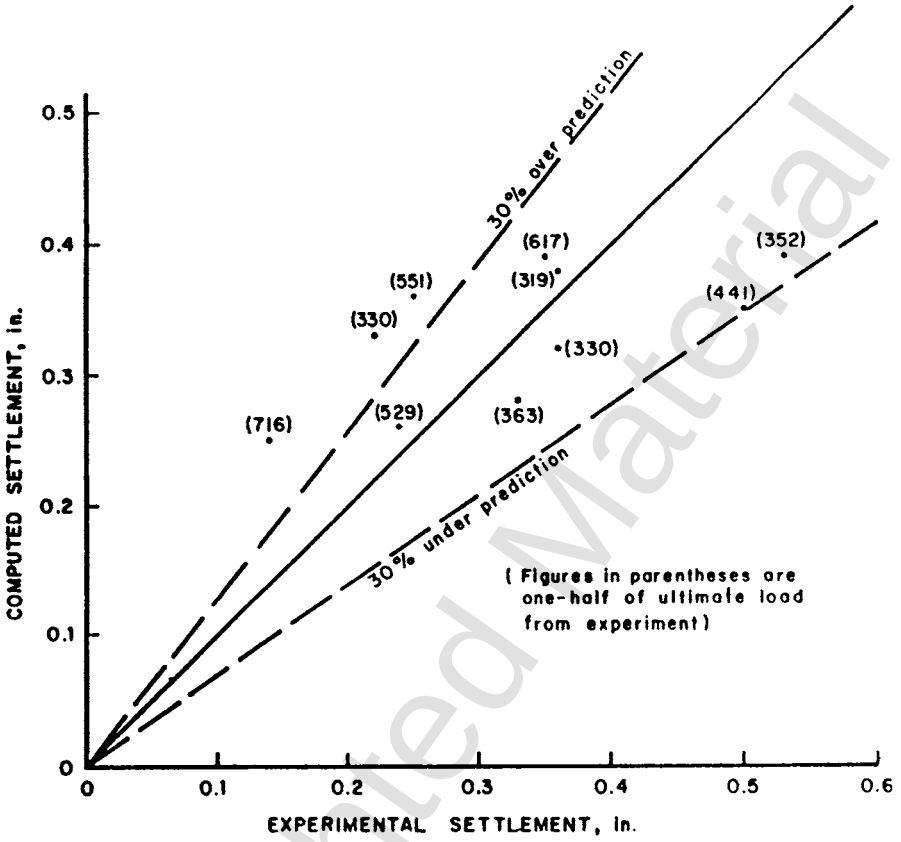

Figure 10.22 Comparison of experimental and computed settlement of axially loaded piles at one-half load capacity (after Minami, 1983).

The information presented here relates to short-term settlement. Settlement due to the consolidation of soft clay must be computed separately and added to the short-term settlement. Long-term settlement of cohesionless soil, perhaps due to vibration, must also be treated separately.

10.6 EXAMPLE PROBLEMS

This example is included to illustrate a common case for a bridge foundation. The soil deposit consists of two sublayers. The top layer is 5-m stiff clay underlain by a dense sand layer. The proposed pile for foundations is prestressed concrete pile with a 0.45-m (18-in.) outside diameter. The elastic modulus of the prestressed pile is 31,000,000 kPa. Each pile is required to be driven to 20 m below the ground surface. The soil properties interpreted from the geotechnical investigation report can be summarized as follows:

Layer I consists of tan to brown stiff clay; its thickness is about 5 m. Based on unconfined compressive tests conducted in the laboratory, the stiff clay has an unconfined-compressive strength of 95 kN/m^2. The unit weight of the soil is 18.9 kN/M^3. The PI for the clay is about 15, which indicates insignificant expansive properties.

Layer II consists of brown silty dense sand to sandy gravel; its total thickness is about 25 m. The fine to coarse sand has a blow counts ranging from 23 to 28. The estimated internal friction angle based on the blow counts is 36°. The unit weight of the soil is 19.1 kN/M^3. The water table is at the top of the sand layer.

10.6.1 Skin Friction

The general equation for skin friction is

$$Q_s = \Sigma f A_s \tag{10.39}$$

Skin Friction from Layer I—Stiff Clay (0 to 5 M)

API Method

$$fA_s \text{ (clay)} = \alpha c \pi B h \tag{10.40}$$

where

Avg. effective overburden pressure (p) is 18.9 * 2.5 = 47.3 kN/m^2,
$\alpha = (0.5)\ (c/p)^{-0.25} = (0.5)\ (95/47.3)^{-0.25} = 0.42$ (from Eq. 10.6)
fA_s (clay) = (0.42) (95)*π *(0.45)* (5) = 282 kN

FHWA Method

$$\begin{aligned} fA_s\ (clay) &= \alpha c_u \pi B h \\ &= (0.72)(95)\pi(0.45)(5) \\ &= 483 \text{ kN} \end{aligned} \tag{10.41}$$

U.S. Army Corps Method

$$\begin{aligned} fA_s \text{ (clay)} &= \alpha c_u \pi B h \\ &= (0.5)(95)\pi(0.45)(5) \\ &= 335 \text{ kN} \end{aligned} \tag{10.42}$$

Skin Friction from Layer II—Dense Sand (5 to 20 M)

Avg. effective overburden pressure (p) from 0 to 5 m (18.9)(2.5) = 47.3 kN/m^2,

Avg. effective overburden pressure (p) from 5 to 10 m (18.9(5) + (9.1)(2.5) = 117.3 kN/m^2,

Avg. effective overburden pressure (p) from 10 to 15 m (18.9)(5) + (9.1)(7.5) = 162.8 kN/m^2, and

Avg. effective overburden pressure (p) from 15 to 20 m (18.9)(5) + (9.1)(12.5) = 208.3 kN/m^2.

API Method

$$fA_s\ (sand) = k_0 \sum (\gamma h)\tan(\phi - 5)\pi Bh \tag{10.43}$$

FHWA Method

ω (taper angle) = 0.0 (because of a uniform pile section)

$$fA_s\ (sand) = k_0 C_f \sum (\gamma h)\sin(\delta)\pi Bh \tag{10.44}$$

The average displaced volume per foot is $\pi(0.45)^2/4 = 0.159$ m^3.
For a precast concrete pile with $V = 0.159$ m^3, $\delta = 0.9\phi$.

U.S. Army Corps Method

$$fA_s(\text{sand}) = k_0 \sum (\gamma h)\tan(\delta)\pi Bh \tag{10.45}$$

Skin friction in sand increases linearly to an assumed critical depth, D_c.
$D_c = 20B = 20(0.45) = 9$ m for dense sand.

TABLE 10.8 Computation of Skin Friction from Each Sublayer Based on the API Method

(1) Depth Interval	(2) Total Area (πBh)	(3) Average Effective Stress	(4) $k_0 \tan(\phi - 5)$ $k_0 = 1$, $\phi = 36$	(5) fA_s = (2)*(3)*(4)
5–10 m	7.07 m^2	117.3 kN/m^2	0.6	497.6 kN
10–15 m	7.07 m^2	162.8 kN/m^2	0.6	690.6 kN
15–20 m	7.07 m^2	208.3 kN/m^2	0.6	883.6 kN
				ΣfA_s = 2071.8 kN

TABLE 10.9 Computation of Skin Friction from Each Sublayer Based on the FHWA Method

(1) Depth Interval	(2) Total Area (πBh)	(3) Average Effective Stress	(4) $k_0 C_f \sin(\delta)$ $k_0 = 2.1$, $\delta = 0.9\phi$, $C_f = 0.95$	(5) fA_s = (2)*(3)*(4)
5–10 m	7.07 m^2	117.3 kN/m^2	1.07	887.4 kN
10–15 m	7.07 m^2	162.8 kN/m^2	1.07	1231.6 kN
15–20 m	7.07 m^2	208.3 kN/m^2	1.07	1575.8 kN
				ΣfA_s = 3694.8 kN

Average effective overburden pressure p from 5 to 9 m (18.9)(5) + (9.1)(2) = 112.7 kN/m^2.

Effective overburden pressure p at 9 m (18.9)(5) + (9.1)(4) = 130.9 kN/m^2.

TABLE 10.10 Computation of Skin Friction from Each Sublayer Based on the U.S. Army Corps Method

(1) Depth Interval	(2) Total area (πBh)	(3) Average Effective Stress	(4) $k_0 \tan \delta$ $k_0 = 2$, $\delta = 0.9\phi$	(5) fA_s = (2)*(3)*(4)
5–9 m	5.66 m^2	112.7 kN/m^2	1.27	810.1 kN
9–20 m	15.55 m^2	Critical depth control 130.9 kN/m^2	1.27	2585.1kN
				ΣfA_s = 3395.1 kN

End Bearing

API Method. The general equation for end bearing is

$$Q_p = N_q \sigma_v A_p \tag{10.46}$$

where

A_p (tip area) = (0.45) (0.45) (π/4) = 0.159 m^2,
σ_v (effective stress at tip) = (18.9) (5) + (9.1) (15) = 231 kN/m^2, and
N_q = 40.

$$Q_p = (40)(231)(0.159) = 1469$$

FHWA Method. The general equation for end bearing is

$$Q_p = \alpha N_q \sigma_v A_p \tag{10.47}$$

where

$$\begin{aligned} A_p \text{ (tip area)} &= (0.45)\ (0.45)\ (\pi/4) = 0.159 \text{ m}^2, \\ \sigma_v \text{ (effective stress at tip)} &= (18.9)\ (5) + (9.1)\ (15) = 231 \text{ kN/m}^2, \\ N_q &= 60, \\ \alpha &= 0.7, \text{ and} \end{aligned}$$

The limiting value from Meyerhof (1976) is 7258 kN/m^2.

$$Q_p = (0.7)\ (60)\ (231) = 9702 > 7258 \text{ kN/m}^2$$

Therefore, the limiting value should be used for the bearing capacity.

$$Q_p = (7258)(0.159) = 1154$$

U.S. Army Corps Method. The general equation for end bearing is

$$Q_p = N_q \sigma_v A_p \tag{10.48}$$

where

$$\begin{aligned} A_p \text{ (tip area)} &= (0.45)\ (0.45)\ (\pi/4) = 0.159 \text{ m}^2, \\ \sigma_v \text{ (effective stress at } D_c) &= (18.5)\ (5) + (9.1)\ (4) = 130.9 \text{ kN/m}^2, \text{ and} \\ N_q &= 45. \end{aligned}$$

$$Q_p = (45)\ (130.9)\ (0.159) = 936$$

Total Bearing Capacity

API Method. The total bearing capacity of the pile is given in Eq. 10.49. To determine the total bearing capacity of the pile, the value from the skin friction equations (Eqs. 10.40 and 10.43) and the end-bearing equation (Eq. 10.46) must be used in Eq. 10.49.

$$Q_{\text{total}} = Q_s + Q_p = (282 + 2{,}071) + 1{,}469 = 3{,}822 \text{ kN} \tag{10.49}$$

FHWA Method. The total bearing capacity of the pile is given in Eq. 10.50. To determine the total bearing capacity of the pile, the values from the skin friction equations (Eqs. 10.41 and 10.44) and the end-bearing equation (Eq. 10.47) must be used in Eq. 10.49.

$$Q_{\text{total}} = Q_s + Q_p = (483 + 3695) + 1154 = 5332 \text{ kN} \tag{10.50}$$

U.S. Army Corps Method. The total bearing capacity of the pile is given in Eq. 10.51. To determine the total bearing capacity of the pile, the value from the skin friction equations (Eqs. 10.42 and 10.45) and the end-bearing equation (Eq. 10.48) must be used in Eq. 10.49.

$$Q_{\text{total}} = Q_s + Q_p = (335 + 3395) + 936 = 4666 \text{ kN} \qquad (10.51)$$

The values of pile capacity shown above, computed by three different methods, vary significantly. The engineer may select an average value, or the lowest value, or make a decision based on the perceived validity of the three methods. Recommending a field load test may be justified for a large job.

10.7 ANALYSIS OF PILE DRIVING

10.7.1 Introduction

Ever since engineers began using piles to support structures, attempts have been made to find rational methods for determining the load a pile can carry. Methods for predicting capacities were proposed using dynamic data obtained during driving. The only realistic measurement that could be obtained during driving was pile set (blow count); thus, concepts equating the energy delivered by the hammer to the work done by the pile as it penetrates the soil were used to obtain pile-capacity expressions, known as *pile formulas.*

Up to the late 19th century, the design of piling was based totally on prior experience and rule-of-thumb criteria. One of the first attempts at theoretical evaluation of pile capacity was published in *Engineering News* under ''Piles and Pile Driving,'' edited by Wellington in 1893. This approach is still known today as the *Engineering News pile-driving formula.* Since Wellington proposed the well-known Engineering News Formula in 1893, a number of other attempts have been made to predict the capacity of piles, and many reports of field experience have become available. Because of their simplicity, pile formulas have been widely used for many years. However, statistical comparisons with load tests have shown poor correlations and wide scatter. As a result, except where well-supported empirical correlations under a given set of physical and geologic conditions are available, pile formulas should be used with caution.

Another approach to modeling a pile during driving involves the use of the wave-equation method. The application of wave-equation analysis in pile driving has been of great interest to engineers for many years. Not only does this method provides better information on load capacity than other dynamic methods, but the wave equation will yield stresses in the pile during driving. The wave-equation method is a semitheoretical method whose reliability in predicting bearing capacity and driving stress depends primarily on the ac-

curacy of the parameters defining pile and soil properties. However, the wave-equation method has been compared with a number of results of actual field tests performed throughout the world, and the results show that this method is rational and reliable.

The following sections provide a brief review of the conventional dynamic formulas and discuss the problems associated with them. The wave-equation method will also be described briefly.

10.7.2 Dynamic Formulas

The simplest form of dynamic formulas in use today is based on equating the energy used to the work done when a pile is moved a certain distance (set) against soil resistance. Various methods have been used to evaluate the many variables that could affect the results of a dynamic formula. In general, there is no indication that the more elaborate formulas are more reliable or that any one dynamic formula is equally applicable to all types of piles under all soil conditions. The driving formulas were all derived using grossly simplified assumptions.

Pile-driving formulas are based on the assumption that the bearing capacity of a driven pile is a direct function of the energy delivered to it during the last blows of the driving process, and that the energy from the hammer to the pile and soil is transmitted instantaneously on impact. These two assumptions have been proven wrong by many investigators. Researchers have clearly demonstrated that the bearing capacity of a pile is related less to the total hammer energy (per blow) than to the distribution of this energy with time during the driving process. Data on pile driving using wave-propagation theory indicate that time effects related to the propagation of the impact forces in the pile govern the behavior of piles during driving. The lack of confidence in dynamic formulas is demonstrated by the fact that the safety factors applied to determine the allowable loads are always very large. For example, a nominal value of 6 is used for the safety factor in the Engineering News Formula.

Most dynamic formulas yield the ultimate pile capacity rather than the allowable or design capacity. Thus, the specified design load should be multiplied by a factor of safety to obtain the ultimate pile capacity that is inputted in to the formula to determine the required *set* (amount of pile penetration per blow).

The equations used in two of the dynamic formulas are shown below. If the formula is in terms of allowable (design) pile capacity, then a factor of safety is already included in the formula and the application of an additional safety factor is not required. Equations 10.51 to 10.53 show several variations of the commonly used Engineering News Formula. Any consistent set of units may be used for formulas unless noted otherwise.

Engineering News Record:

$$P_u = \frac{W_r \cdot h}{s + 1.0} \quad \text{for drop hammers } (h \text{ and } s \text{ both in ft}) \qquad (10.52)$$

$$P_u = \frac{W_r \cdot h}{s + 0.1} \quad \text{for steam hammers } (h \text{ and } s \text{ both in ft}) \qquad (10.53)$$

$$P_a = \frac{2 \cdot W_r \cdot h}{s + 0.1} \quad \text{for steam hammers } (h \text{ in ft, } s \text{ in inches}) \qquad (10.54)$$

AASHTO (1983)

$$P_a = \frac{2 \cdot h \cdot (W_r + A_r \cdot P)}{s + 0.1} \quad \text{for double-acting steam hammers } (h \text{ in ft, } s \text{ in inches}) \qquad (10.55)$$

A factor of safety of 6 is included in Eqs. 10.54 and 10.55. The following is a list of symbols used for the pile formulas.

A_r = ram cross-sectional area,
h = height of ram fall,
P_u = ultimate pile capacity,
P_a = allowable pile capacity (with a factor of safety = 6),
p = steam (or air) pressure,
s = amount of point penetration per blow, and
W_r = weight of ram (for double-acting hammers, includes weight of casing).

10.7.3 Reasons for the Problems with Dynamic Formulas

The problems associated with pile-driving formulas can be related to each component within the pile-driving process: the driving system, the soil, and the pile. An investigation of these parameters indicates three reasons why the formulas lack validity.

First, the derivation of most formulas is not based on a realistic treatment of the driving system because they fail to consider the variability of equipment performance. Typical driving systems can include many elements in addition to the ram, such as the helmet (drive cap), cap block (hammer cushion), pile cushion, and anvil. These components affect the distribution of the hammer energy with time, both at and after impact, which influences the magnitude and duration of peak force. The peak force determines the ability of the hammer system to advance piles into the soil.

Second, the soil resistance is very crudely treated by assuming that it is a constant force. This assumption neglects even the most obvious characteristics

of real soil performance. Dynamic soil resistance, or resistance of the soil to rapid pile penetration produced by a hammer blow, is by no means identical to the static load required to produce very slow penetration of the pile point. Rapid penetration of the pile point into the soil is resisted not only by static friction and cohesion, but also by soil viscosity, which is comparable to the viscous resistance of liquids against rapid displacement under an applied force. The net effect is that the driving process creates resistance forces along the pile shaft and at the pile tip, which are substantially increased because of the high shear rate. The viscous effect tends to produce an apparent increase in soil resistance, which is evident only under dynamic conditions.

Third, the pile is assumed to be rigid, and its length is not considered. This assumption completely neglects the flexibility of the pile, which reduces its ability to penetrate soil. The energy delivered by the hammer sets up time-dependent stresses and displacements in the pile-head assembly, in the pile, and in the surrounding soil. In addition, the pile behaves not as a concentrated mass, but as a long elastic bar in which stresses travel longitudinally as waves. Compressive waves that travel to the pile tip are responsible for advancing the pile into the ground.

10.7.4 Dynamic Analysis by the Wave Equation

As discussed in the previous section, dynamic formulas do not yield acceptably accurate predictions of actual pile capacities and provide no information on stresses in the piles. The one-dimensional wave-equation analysis has eliminated many shortcomings associated with pile formulas by providing a more realistic analysis of the pile-driving process. The use of the wave-equation method for predicting the behavior of driven piles was employed in 1938 (Glanville et al.). A model was proposed by Smith (1960) as shown in Figure 10.23, and has been discussed and utilized by a number of writers (Samson et al., 1963; Goble et al., 1972; Holloway and Dover, 1978). It appears to describe reasonably well the behavior of the pile during driving if soil parameters are properly selected. The selection of soil parameters has advanced only slightly since the time of Smith's proposal. The existence of residual stresses in a pile after its installation can be explained by the wave-equation model.

Wave equation is a term applied to several computer programs, including TTI by Hirsch et al. (1976), WEAP86 by Goble and Rausche (1986), and GRLWEAP by Pile Dynamics, Inc. (2005), that use a finite-difference method to model dynamic pile behavior. The wave-equation analysis uses wave-propagation theory to model the longitudinal wave transmitted along the pile axis when it is struck by a hammer. As the ram impact occurs, a force pulse is developed in the pile that travels downward toward the pile tip at a constant velocity that depends on the properties of the pile material. When the force pulse reaches the portion of the pile that is embedded, it is attenuated by frictional resistance from the soil along the pile. If the attenuation is incomplete, the force pulse will reach the pile tip and a reflected force pulse, which

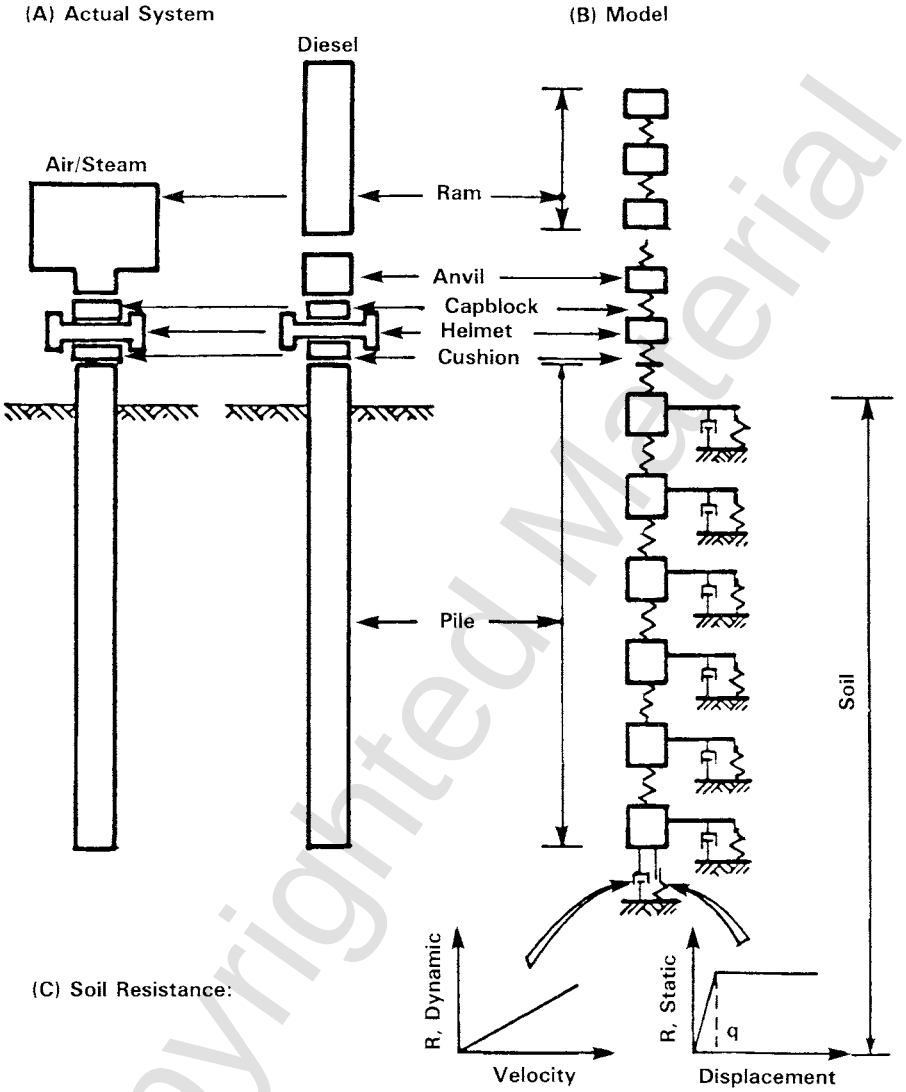

Figure 10.23 Pile-driving model proposed by Smith (1960).

is governed by the tip resistance, is generated. The pile will penetrate into the soil when the peak force generated by the ram impact exceeds the ultimate soil resistance at the pile tip and along the pile. The wave-equation analysis provides two types of information:

1. It provides information on the relationship between pile capacity and driving resistance. The user inputs data on soil side shear and end bearing, and the analysis provides an estimate of the set (inches/blow) under

one blow of the specified hammer. By specifying a range of ultimate pile capacities, the user obtains a relationship between ultimate pile capacity and penetration resistance (blows per inch or blows per foot), as shown in Figure 10.24.

2. The analysis also provides relationships between driving stresses in the pile for a specific soil and penetration resistance, as shown in Figure 10.25.

In summary, the wave-equation analysis enables the user to develop curves of capacity versus blow count for different pile lengths. This information may be used in the field to determine when the pile has been driven sufficiently to develop the required capacity. The analysis is used to (1) select the right combination of driving equipment to ensure that the piles can be driven to the required depth and capacity; (2) design the minimum required pile section for driving; (3) minimize the chances of overstressing the pile; and (4) minimize driving costs.

10.7.5 Effects of Pile Driving

The first and most obvious effect of installing a pile is the displacement of a volume of soil nearly equal to the volume of the pile. While some speculation has occurred about the patterns of such displacement as a pile is progressively driven into the soil, there is no accepted solution that would allow plotting of displacement contours. The volume changes cause distortion of clay and changes in the structure of clay, and usually result in loss of strength of clay. The volume changes during pile driving result in lateral deformations and uplift, and lateral movement can occur in piles previously driven.

If an open-ended-pipe pile is driven into clay, a soil plug may form during the pile driving after a certain pile penetration and may be carried down with the pile as the pile is driven farther. If the plug does not form, the pile will behave as a nondisplacement pile, with heave and lateral displacement being minimized. Pile driving in clay causes increases in total pressure and porewater pressure above the at-rest pressures in the vicinity of the pile wall as the pile tip passes a point. Such increases have been observed in the soil at several diameters away from the pile, with the effect being analogous to the increase in temperature of a slab due to the imposition of a line source of heat. Observations indicate that a significant dynamic effect occurs in the porewater continuum during impact, with sudden and sizable increases in these quantities occurring as a result of a hammer blow. A porewater-pressure gauge was embedded in the soil about 15 diameters away from the point where a 6-in. (15-cm) pile was being driven. There was a sudden jump in the pressure-gauge reading with each blow of a drop hammer.

An obvious effect of pile driving is a shearing deformation of large magnitude as the pile wall moves past a particular point in the soil. At present, it is not clear whether all of the shearing deformation occurs at the interface

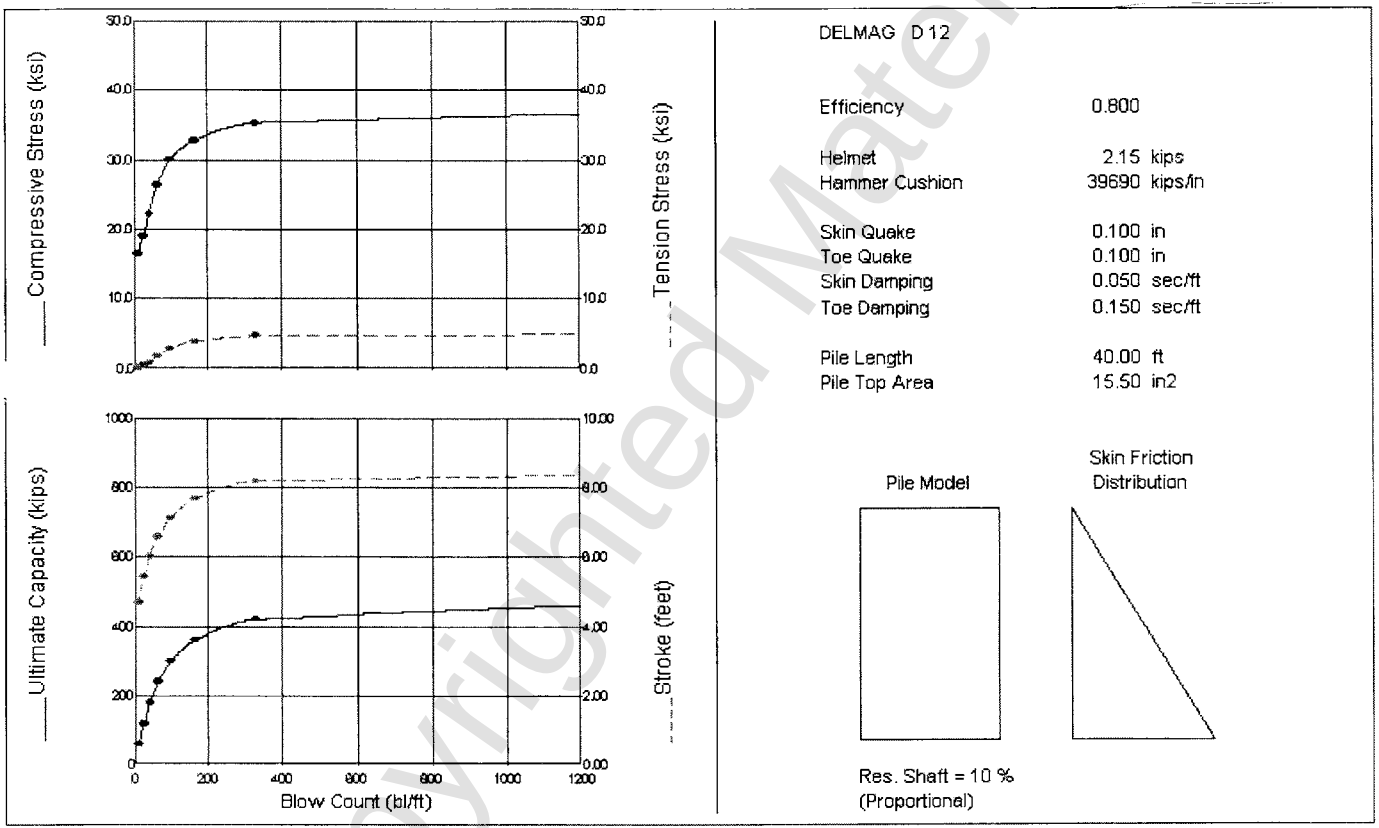

Figure 10.24 Relationship between pile capacity and driving resistance.

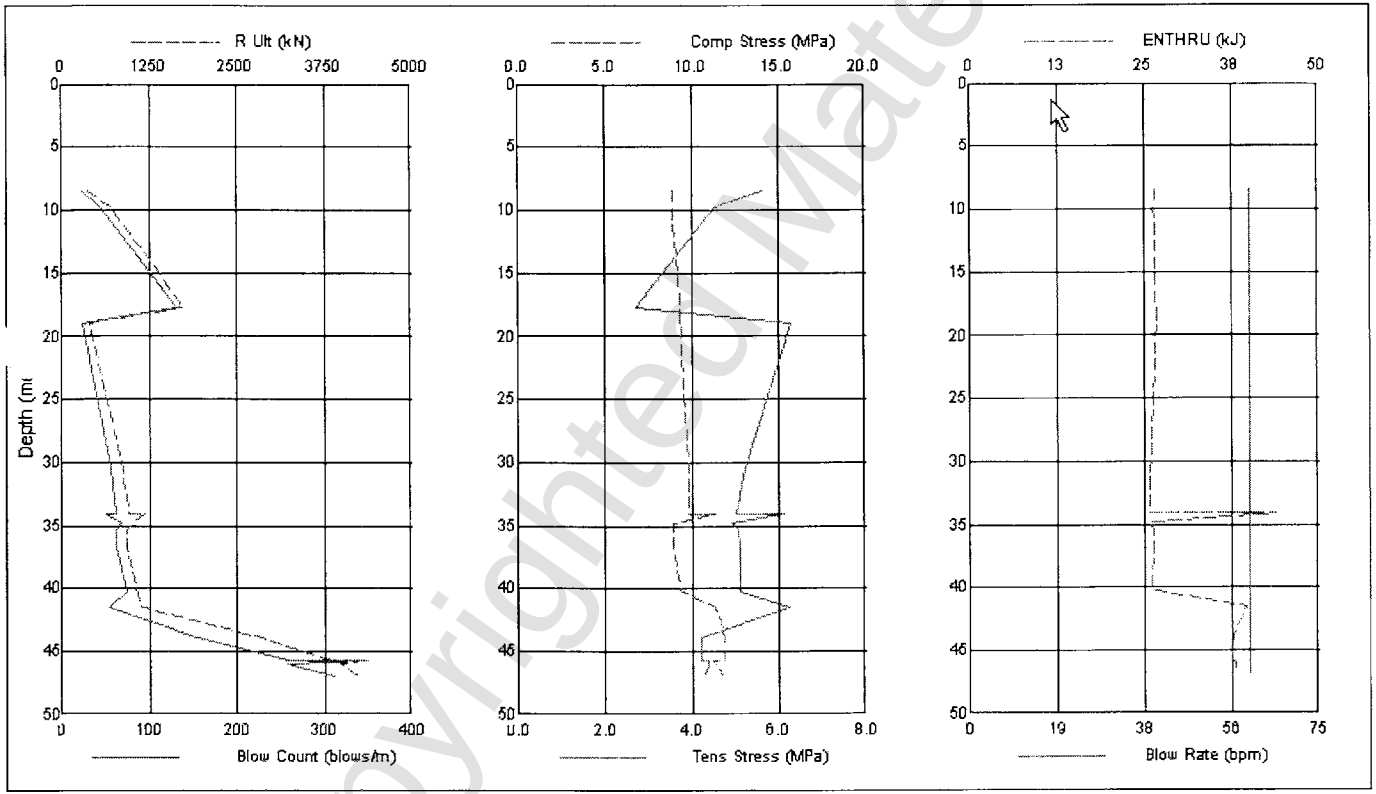

Figure 10.25 Relationship between driving stress and pile penetration.

between the pile and the soil or whether some soil moves down with the pile. In regard to downward movement of an upper stratum of soil, Tomlinson (1980) reported that driving a pile causes a significant amount of soil in an upper stratum to move into the stratum just below. At the completion of driving there will be a stress in the soil that is indeterminate, probably complex, and completely different from the in situ state of stress. The state of stress immediately after driving will reflect the residual stresses in the pile that exist on completion of driving.

10.7.6 Effects of Time After Pile Driving with No Load

Cohesive Soil Because of the time required for excess porewater stress to dissipate in soils with low permeability, there are significant effects over time on piles driven into saturated clays. An increase in axial capacity occurs over time for such piles. Engineers have long been aware that the piles ''set up'' over time and that this effect can be quite dramatic. There are reports of pile-driving crews stopping for lunch with a pile moving readily; when they began driving after lunch, the pile had set up so that is refused to drive farther. Dr. Karl Terzaghi was called to a location where it was impossible to drive piles. The piles were timber and were designed to carry a relatively light load. The caller reported that it was difficult to drive the piles to grade, that they floated up after each hammer blow, and that their bearing capacity was quite small. Terzaghi asked that the piles be driven to grade and deliberately delayed going to the site. After finally arriving at the site, he directed load tests to be performed. It was found that the piles were performing satisfactorily.

The state of stress of clay immediately after pile driving is such that there are excess porewater pressures that are undoubtedly at a maximum in the vicinity of the pile wall, but measurements have shown that these excess porewater pressures extend several diameters, and perhaps more, away from the pile wall. The excess porewater pressures decay relatively rapidly where gradients are high, with the decay being an exponential function of time. Along with the decay of excess porewater pressures is movement of water in the clay, with evidence indicating that its flow is predominantly horizontal. The horizontal movement of water leads to a decrease in water content at the pile wall; measurements have indicated that this change in water content is significant. Along with the decrease in water content, an increase in the shearing strength of the clay occurs. The process is complex and not well understood because it seems to indicate an exchange between equal volumes of solids and water. Part of the strength increase may be due to the thixotrophy of the clay.

Along with the movement of water due to the excess porewater pressures created by pile driving, there is consolidation of the clay due to its own weight. The remolding of the clay due to pile driving changes its consolidation characteristics so that the soil consolidates under its own weight, with the result that the ground surface tends to move down. If the ground surface

moves down, negative skin friction tends to develop at the pile wall, with a consequent change in the residual stresses that existed immediately after pile driving.

Cohesionless Soil Driving a pile into sand or cohesionless soil, with the resulting vibration, causes the sand deposit to decrease in volume sufficiently to allow the pile to penetrate. The volume decrease is frequently such that the ground surface is lowered, particularly in the vicinity of the pile. While there are few experimental data, there is a strong indication that the lateral vibration of a pile driven into sand results in arching. A particle of sand will move outward and downward. Lateral vibration creates a space that is slightly larger than the pile, and arching reduces the lateral stress against the pile wall. Therefore, the soil stresses against the wall of a pile in sand are usually much lower than passive pressures and can be lower than the earth pressure at rest.

If the sand is so dense that volume change cannot take place, the driving resistance becomes extremely high and crushing of the sand grains will result. The above points apply principally to a sand composed of quartz or feldspar; a pile driven into calcareous sand will crush the sand, and lateral earth pressures against the pile wall can be quite low, especially if the calcareous sand is cemented. It is usually assumed that an open-ended-pipe pile driven into quartz sand will plug; this may not be the case for calcareous sand. As with clay, driving a pile into cohesionless soil will cause shearing deformation of a large magnitude at the pile wall; sand above a clay can be moved downward; there will be residual stresses in the driven pile; and there will be a complex state of stress in the soil surrounding the pile after the pile has been driven.

PROBLEMS

P10.1. A steel pile has an outer diameter (OD) of 1.0 m and an inner diameter (ID) of 0.86 m. The subsurface condition consists mainly of cohesionless soils, and the pile was driven to a depth of 33.3 m. The total unit weight of soils is 18 kN/m^3 and the internal friction angle is 32° at the ground surface and linearly increases to 38° at a depth of 40 m. The water table is 10 m below the ground surface. Compute the ultimate axial capacity for this pile.

P10.2. A contractor plans to install a 0.5-m-OD steel pile embedded in cohesive soils. The pile is an open-ended steel pipe, and a plug of soil may be forced up the inside of the pile. The soil resistance from the plug consists of the friction from the plug inside the pile and the bearing capacity from the steel metal area only. The soil resistance from the plug is compared to the resistance from the end bearing over the full area of the base, and the smaller of the two values is used for tip resistance. Use both API method and Lambda methods for com-

putations.

Pile and Soil Data

Pile length: = 39 m
Pile diameter: OD = 0.50 m
ID = 0.48 m

Soil Information

Depth (m)	Soil Type	γ' kN/m^3	C kN/m^2
0–4	Clay	19	9.8
4–10	Clay	9	9.8
10–20	Clay	9	19.6
20–36	Clay	9	58.8
36–40	Clay	9	78.4